Received: 14 July 2022 | Revised: 22 September 2022 | Accepted: 24 September 2022

DOI: 10.1002/wrna.1766

ADVANCED REVIEW

WIREs RNA WILEY

Caught in the act—Visualizing ribonucleases during eukaryotic ribosome assembly

Claudia Schneider[1] | **Katherine E. Bohnsack**[2]

[1]Biosciences Institute, Faculty of Medical Sciences, Newcastle University, Newcastle upon Tyne, UK

[2]Department of Molecular Biology, University Medical Center Göttingen, Göttingen, Germany

Correspondence
Katherine E. Bohnsack, Department of Molecular Biology, University Medical Center Göttingen, Humboldtallee 23, Göttingen 37073, Germany.
Email: katherine.bohnsack@med.uni-goettingen.de

Funding information
Royal Society, Grant/Award Number: RGF\EA\180045; University Medical Centre Göttingen

Edited by: Jeff Wilusz, Editor-in-Chief

Abstract

Ribosomes are essential macromolecular machines responsible for translating the genetic information encoded in mRNAs into proteins. Ribosomes are composed of ribosomal RNAs and proteins (rRNAs and RPs) and the rRNAs fulfill both catalytic and architectural functions. Excision of the mature eukaryotic rRNAs from their precursor transcript is achieved through a complex series of endoribonucleolytic cleavages and exoribonucleolytic processing steps that are precisely coordinated with other aspects of ribosome assembly. Many ribonucleases involved in pre-rRNA processing have been identified and pre-rRNA processing pathways are relatively well defined. However, momentous advances in cryo-electron microscopy have recently enabled structural snapshots of various pre-ribosomal particles from budding yeast (*Saccharomyces cerevisiae*) and human cells to be captured and, excitingly, these structures not only allow pre-rRNAs to be observed before and after cleavage events, but also enable ribonucleases to be visualized on their target RNAs. These structural views of pre-rRNA processing in action allow a new layer of understanding of rRNA maturation and how it is coordinated with other aspects of ribosome assembly. They illuminate mechanisms of target recognition by the diverse ribonucleases involved and reveal how the cleavage/processing activities of these enzymes are regulated. In this review, we discuss the new insights into pre-rRNA processing gained by structural analyses and the growing understanding of the mechanisms of ribonuclease regulation.

This article is categorized under:

Translation > Ribosome Biogenesis

RNA Processing > rRNA Processing

KEYWORDS

ribonuclease, ribosome biogenesis, RNA exosome, RNA processing

1 | INTRODUCTION

All cellular protein synthesis is mediated by ribosomes, conserved ribonucleoprotein complexes (RNPs) composed of RNAs and RPs. The rRNAs endow catalytic function through peptide bond formation as well as forming an architectural scaffold for the complex thus enabling other aspects required for protein production, including tRNA binding and mRNA decoding. The small subunit (SSU, 40S) of eukaryotic cytosolic ribosomes contains the 18S rRNA, while the large subunit (LSU, 60S) contains the 25S (yeast)/28S (human), 5.8S, and 5S rRNAs (Anger et al., 2013; Ben-Shem et al., 2011). The 5S rRNA is independently synthesized by RNA polymerase III and assembled into a 5S RNP complex before recruitment to pre-60S particles (Ciganda & Williams, 2011; Madru et al., 2015). In contrast, the 18S, 5.8S, and 25S/28S rRNAs are co-synthesized as a precursor rRNA, termed 35S (budding yeast)/47S (human). Co-synthesis of three of the four rRNAs ensures equal expression, important for efficient ribosomal subunit production. Within the primary pre-rRNA transcript, the mature rRNAs are flanked and separated by precursor sequences (5′ and 3′ external transcribed spacers (5′/3′ ETS) and internal transcribed spacers 1 and 2 (ITS1 and ITS2); Figure 1).

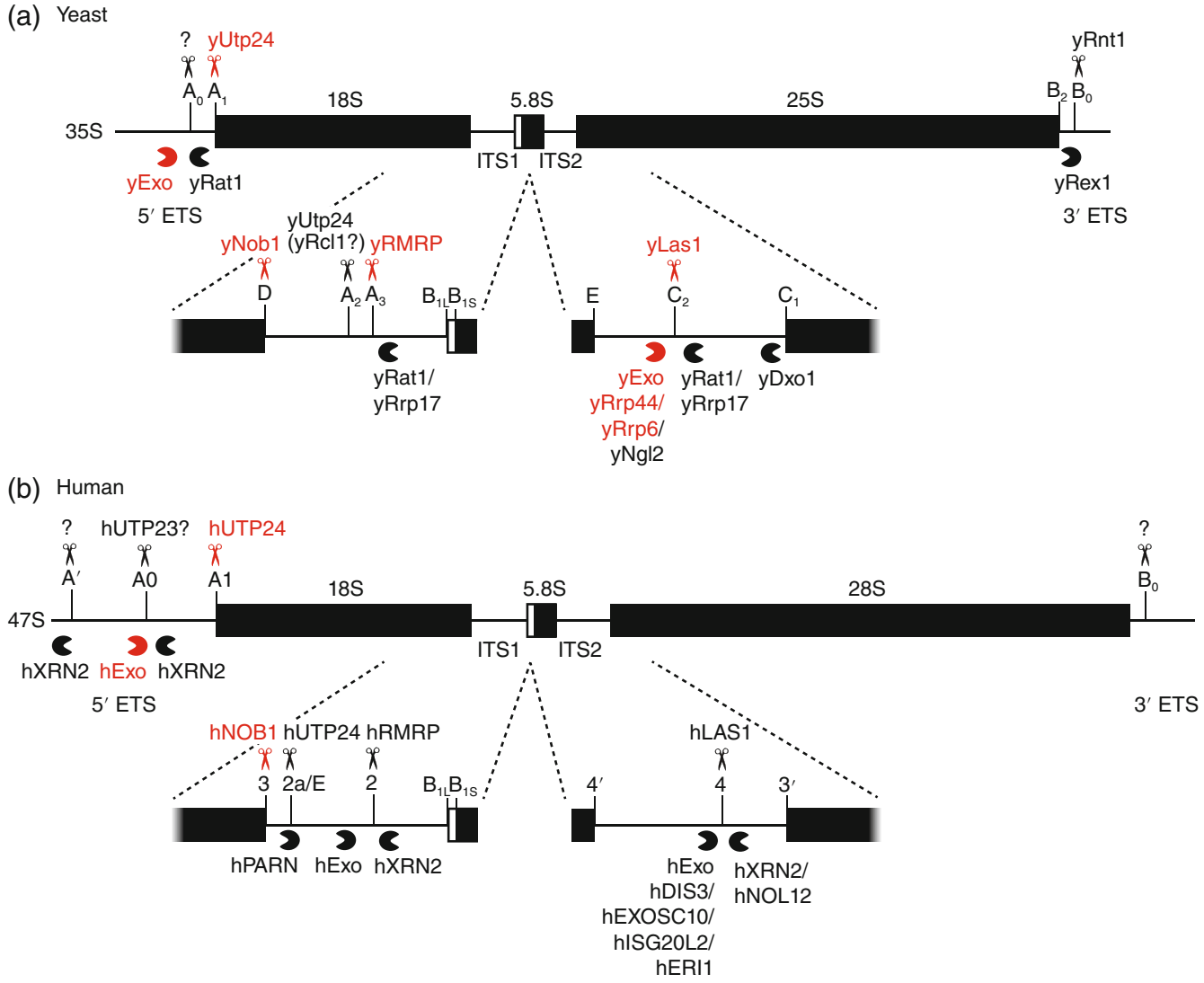

FIGURE 1 Overview of ribonucleases involved in yeast and human pre-rRNA processing. (a,b) Schematic view of full-length pre-rRNA transcripts from budding yeast (*S. cerevisiae*) (35S; a) and humans (47S; b) composed of the mature 18S, 5.8S, and 25S/28S rRNAs (black rectangles) as well as internal and external transcribed spacers (ITS and ETS; black lines). Pre-rRNA cleavage sites are marked by vertical lines and conventional numbers/letters. Endoribonucleases (scissors) responsible for pre-rRNA cleavage events are marked above the transcripts and exoribonucleases (Pacmen) involved in processing steps are shown below. Unknown or candidate enzymes are indicated with "?" and enzymes "captured in action" and discussed in detail in this review are highlighted in red.

Removal of the precursor sequences is accomplished by a series of endoribonucleolytic cleavages and exoribonucleolytic trimming steps, which take place within large pre-ribosomal particles and are intimately coordinated with folding and modification of the rRNA as well as assembly of RPs. Compared to direct endoribonucleolytic cleavage at the mature rRNA ends, the strategy of sequential endoribonucleolytic cleavages coupled to exoribonucleolytic processing provides opportunities for regulation and quality control of the pathway. On the one hand, the timing of consecutive endoribonucleolytic cleavages can be controlled relative to other assembly events and on the other hand, fine-trimming of rRNA ends by exoribonucleases provides a mechanism via which aberrant pre-rRNAs can be efficiently degraded by the processing machinery if subunit assembly is impaired.

Pre-rRNA intermediates present in yeast and human cells are well defined and most pre-rRNA cleavage sites have been accurately mapped. While some pre-rRNA processing events follow a defined sequential order, there is flexibility in other cases and alternative pre-rRNA processing pathways are observed. Perturbation of the pathway or changes in its dynamics, arising, for example, in ribosomopathies and/or different environmental conditions, can lead to alterations in pre-rRNA processing. Many ribonucleases required for pre-rRNA processing have been identified, although some remain elusive. The yeast and human pre-rRNA processing pathways have been described in detail in several excellent reviews (Aubert et al., 2018; Bohnsack & Bohnsack, 2019; Henras et al., 2015; Mullineux & Lafontaine, 2012; Tomecki et al., 2017).

Pre-rRNA processing events are irreversible, committed steps during ribosome assembly and as such, they contribute to driving the directionality of the pathway toward mature subunit formation. Processing events therefore represent valuable checkpoints and key assembly milestones often need to be accomplished to achieve processing competence. Almost all ribonucleases lack inherent target specificity in terms of substrate recognition and catalytic function. Nucleotide-specific pre-rRNA cleavages therefore require strict regulation of their spatial contexts. Momentous advances in cryogenic electron microscopy (cryo-EM) in recent years have enabled numerous structural snapshots of ribosome biogenesis to be captured, providing a wealth of information about pre-ribosome architecture and the factors involved in the assembly process. Excitingly, these structures enable pre-RNA cleavage sites to be observed, as well as the conformation of pre-rRNAs before and after processing events have taken place. Furthermore, they have also enabled various ribonucleases to be visualized together with their pre-rRNA substrates. These structural views provide a new layer of understanding of pre-rRNA processing that goes beyond the identification of the responsible ribonucleases by providing insights into the spatial and temporal contexts of pre-rRNA processing events and the mechanisms by which these critical steps in ribosome assembly are regulated.

2 | RIBONUCLEASES INVOLVED IN EUKARYOTIC PRE-rRNA PROCESSING

The ribonucleases involved in pre-rRNA processing represent a diverse group of enzymes from different families that employ distinct catalytic mechanisms to process and degrade the pre-rRNA in specific ways (Table 1). Some processing steps are mediated by stand-alone endo-/exo-ribonucleases, such as the PIN domain endoribonucleases yUtp24/hUTP24 and yNob1/hNOB1, the 5′-3′ exoribonucleases yRrp17/hNOL12 and yDxo1, the DEDD family 3′-5′ exoribonucleases yRex1-3, hERI1 and hISG20L2, and the RNase III-type endoribonuclease yRnt1. Other processing steps are performed by enzymes that require cofactors, such as the XRN superfamily exoribonuclease yRat1/hXRN2 that is regulated by yRai1/hDOM3Z, or ribonucleases that function in concert with other enzymes, for example, yLas1/hLAS1L and yGrc3/hGRC3. Several aspects of pre-rRNA processing are accomplished by ribonucleases working together in the context of the multiprotein RNA exosome complex. One pre-rRNA cleavage event is catalyzed by a ribozyme, RNase MRP. Due to their critical roles during ribosome assembly, perturbations in ribonucleases involved in pre-rRNA processing are often associated with disease (Table 1). In Sections 2.1 and 2.2, we provide more detailed views on two complex ribonucleolytic machineries involved in pre-rRNA processing, the RNA exosome and RNase MRP.

2.1 | The RNA exosome

The RNA exosome is a multi-subunit RNA degradation machinery evolved from the bacterial degradosome PNPase that is involved in the processing and degradation of a wide variety of RNAs, including pre-rRNAs (Gudipati et al., 2012; Hojka-Osinska et al., 2021; Mitchell et al., 1997; Schneider et al., 2012; Sloan et al., 2012; Szczepińska et al., 2015;

TABLE 1 Ribonucleases involved in pre-rRNA processing

Yeast ribonuclease	Human homolog	Family	Activity	Pre-rRNA processing event	Selected PDB structures (http://rcsb.org/)	Disease associations (https://omim.org/)	References
yRrp44 (exosome)	hDIS3/hDIS3L1 (exosome, hEXOSC1-9)	PIN/RNase II/R	endo/processive 3′-5′ exo	Yeast 5′ ETS removal, 5.8S 3′ end formation; human 5′ ETS + ITS1 removal, 5.8S 3′ end formation	7AJU, 7AJT, 6LQS, 7D4I, 6FSZ, 6H25, 6D6R, 6D6Q, 5VZJ, 5K36, 5C0X, 5C0W	MIM: 607533 (hDIS3) MIM: 614183 (hDIS3L1) Multiple myeloma (MM) Acute myeloid leukemia (AML) Chronic lymphocytic leukemia (CLL) MIM: 606493 (hEXOSC1) Pontocerebellar hypoplasia, type 1F (PCH1F) MIM: 602238 (hEXOSC2) Short stature, hearing loss, retinitis pigmentosa and distinctive facies (SHRF) MIM: 606489 (hEXOSC3) Pontocerebellar hypoplasia, type 1B (PCH1B) MIM: 606492 (hEXOSC5) Cerebellar ataxia, brain abnormalities and cardiac conduction defects (CABAC). MIM: 606019 (hEXOSC8) Pontocerebellar hypoplasia, type 1C (PCH1C)	(Alderuccio et al., 1991; Beheshtian et al., 2019; Bizzari et al., 2020; Boczonadi et al., 2014; Burns et al., 2018; Calame et al., 2021; Chapman et al., 2011; Di Donato et al., 2016; Ding et al., 2012; Dziembowski et al., 2007; Kobyłecki et al., 2018; Lebreton et al., 2008; Lorentzen et al., 2008; Preti et al., 2013; Sakamoto et al., 2021; Schaeffer et al., 2009; Schneider et al., 2007; Schneider et al., 2009; Slavotinek et al., 2020; Sloan et al., 2013; Sloan et al., 2014; Somashekar et al., 2021; Staals et al., 2010;

TABLE 1 (Continued)

Yeast ribonuclease	Human homolog	Family	Activity	Pre-rRNA processing event	Selected PDB structures (http://rcsb.org/)	Disease associations (https://omim.org/)	References
						MIM: 606180 (hEXOSC9) Pontocerebellar hypoplasia, type 1D (PCH1D) Polymyositis-scleroderma overlap syndrome (PMSCL)	Tafforeau et al., 2013; Tomecki et al., 2010; Tomecki et al., 2014; Wan et al., 2012)
yRrp6 (exosome)	hEXOSC10 (exosome)	DEDD (RNase D)	Distributive 3′-5′ exo	Yeast 5.8S 3′ end formation; human 5′ ETS + ITS1 removal, 5.8S 3′ end formation	7MQA, 7AJU, 7AJT, 6LQS, 7D4I, 6FSZ, 6H25, 6D6R, 6D6Q, 5VZJ, 5K36, 5C0X, 5C0W, 4OO1	MIM: 605960 Polymyositis-scleroderma overlap syndrome (PMSCL)	(Blüthner & Bautz, 1992; Briggs et al., 1998; Januszyk et al., 2011; Preti et al., 2013; Sloan et al., 2013; Sloan et al., 2014; Tafforeau et al., 2013)
	hUTP23 (?)	PIN	Endo (?)	human A0 (?)	4MJ7		(Bleichert et al., 2006; Lu et al., 2013; Wells et al., 2017)
yUtp24	hUTP24	PIN	Endo	Yeast $A_1 + A_2$; human A1 + 2a/E	7MQA, 7MQ8, 7MQ9, 7AJU, 7AJT, 6RXZ, 6RXY, 6RXX, 6RXV, 6RXU, 6RXT, 6ZQG, 6ZQF, 6ZQE, 6ZQD, 6ZQC, 6ZQB, 6ZQA, 7D4I, 7D5S, 7D5T, 7D63, 6LQV, 6LQU, 6LQT, 6LQS, 6LQP, 6KE6, 5YZ4, 5TZS, 5WLC, 6ND4, 5OQL, 5JPQ		(An et al., 2018; Bleichert et al., 2006; Tomecki et al., 2015; Wells et al., 2016)
yNob1	hNOB1	PIN	Endo	Yeast D; human 3	6ZV6, 6ZUO, 6ZXF, 6ZXE, 6ZXD, 6G5I,		(Fatica et al., 2003; Fatica et al., 2004; Pertschy

(Continues)

TABLE 1 (Continued)

Yeast ribonuclease	Human homolog	Family	Activity	Pre-rRNA processing event	Selected PDB structures (http://rcsb.org/)	Disease associations (https://omim.org/)	References
					6G53, 6G51, 6G4S, 6G18		et al., 2009; Preti et al., 2013; Sloan et al., 2013; Sloan et al., 2019)
	hPARN	DEDD (CAF1)	Processive 3′-5′ exo	Human ITS1 removal	3D45, 2A1S, 2A1R	MIM: 604212 Autosomal recessive dyskeratosis congenita 6 Telomere-related pulmonary fibrosis and/or bone marrow failure 4	(Dhanraj et al., 2015; Montellese et al., 2017; Stuart et al., 2015; Tummala et al., 2015; Wu et al., 2005; Wu et al., 2009)
yRcl1 (?)	hRCL1 (?)	RNA cyclase-like	Endo (?)	Yeast A_2 (?) human 2a/E (?)	7MQA, 7MQ8, 7MQ9, 7AJU, 7AJT, 6ZQG, 6ZQF, 6ZQE, 6ZQD, 6ZQC, 6ZQB, 6ZQA, 7D4I, 7D5S, 7D5T, 7D63, 6LQV, 6LQU, 6LQT, 6LQS, 6LQP, 6KE6, 5TZS, 5WLC, 5WYK, 5WYJ, 5JPQ, 3PQV		(Billy et al., 2000; Horn et al., 2011; Tanaka et al., 2011)
yNme1 (RNase MRP)	hRMRP (RNase MRP)	Catalytic ncRNA; ribozyme	Endo	Yeast A_3; human 2	7C7A, 6W6V, 7C79	MIM: 157660 (hRMRP) Cartilage-hair hypoplasia (CHH) Metaphyseal dysplasia without hypotrichosis (MDWH) Anauxetic dysplasia 1 MIM: 602486 (hPOP1) Anauxetic dysplasia 2 Connective tissue diseases MIM: 606116 (hPOP3/hRPP38)	(Barraza-García et al., 2017; Bonafé et al., 2002; Chu et al., 1994; Eder et al., 1997; Elalaoui et al., 2016; Glazov et al., 2011; Goldfarb & Cech, 2017; Lan et al., 2020; Lygerou et al., 1994; Lygerou et al., 1996;

TABLE 1 (Continued)

Yeast ribonuclease	Human homolog	Family	Activity	Pre-rRNA processing event	Selected PDB structures (http://rcsb.org/)	Disease associations (https://omim.org/)	References
						MIM: 606115 (hRPP1/hRPP30) Scleroderma	Perederina et al., 2020; Ridanpää et al., 2001; Robertson et al., 2022; Schmitt & Clayton, 1993; Thiel et al., 2005)
yRat1	hXRN2	XRN	Processive 5′-3′ exo	Yeast 5′ ETS removal, 5.8S + 25S 5′ end formation; human 5′ ETS removal, 5.8S + 28S 5′ end formation	3FQD, 7OPK		(Chang et al., 2011; Henry et al., 1994; Jinek et al., 2011; Overbeck et al., 2022; Petfalski et al., 1998; Preti et al., 2013; Sloan et al., 2013; Sloan et al., 2014; Xiang et al., 2009)
yRrp17	hNOL12	RRP17	5′-3′ exo	Yeast 5.8S + 25S 5′ end formation; human 28S 5′ end formation			(Oeffinger et al., 2009; Scott et al., 2017; Sloan et al., 2013)
yRex1-3		DEDD	3′-5′ exo	Yeast 5S, 5.8S + 25S 3′ end formation			(Daniels et al., 2022; van Hoof et al., 2000)
yNgl2		ExoIII/HAP1	3′-5′ exo	Yeast 5.8S 3′ end formation			(Faber et al., 2002; Thomson & Tollervey, 2010)
	hERI1	DEDD (RNase T)	3′-5′ exo	Human 5.8S 3′ end formation	4L8R, 4QOZ		(Ansel et al., 2008; Gabel & Ruvkun, 2008; Pirouz et al., 2019; Tan et al., 2013)

(Continues)

TABLE 1 (Continued)

Yeast ribonuclease	Human homolog	Family	Activity	Pre-rRNA processing event	Selected PDB structures (http://rcsb.org/)	Disease associations (https://omim.org/)	References
yRex4 (indirect role)	hISG20L2	DEDD	3′-5′ exo	Yeast 5.8S 3′ end formation (likely indirect role); human 5.8S 3′ end formation			(Coute et al., 2008; Eppens et al., 2002; Faber et al., 2004)
yLas1	hLAS1L	HEPN	Endo	Yeast C_2; human 4	6OF4, 6OF2, 6OF3	MIM: 300964 Wilson–Turner syndrome Spinal muscular atrophy with respiratory distress (SMARD)	(Butterfield et al., 2014; Castle et al., 2010; Castle et al., 2012; Castle et al., 2013; Gasse et al., 2015; Pillon et al., 2017; Pillon et al., 2019; Schillewaert et al., 2012; Stembalska et al., 2022; Wilson et al., 1991)
yDxo1		Dxo1/Rai1/DXO	5′-3′ exo	Yeast 25S 5′ end formation	6WUK		(Hurtig & van Hoof, 2022)
yRnt1		RNase III	Endo	Yeast B_0	5T16, 4OOG		(Elela et al., 1996; Kufel et al., 1999; Liang et al., 2014; Song et al., 2017)

Zinder & Lima, 2017). The core exosome in budding yeast and human cells is composed of nine catalytically inactive subunits arranged into a hexameric barrel structure with a trimeric cap (Bonneau et al., 2009; Gerlach et al., 2018; Liu et al., 2006; Makino et al., 2013; Makino et al., 2015).

The dual-function ribonuclease yeast (y)Rrp44 (Table 1) endows the yeast complex with processive 3′-5′ exoribonucleolytic activity through its RNase II/R catalytic (RNB) domain and endoribonucleolytic activity via its N-terminal PilT N-terminus (PIN) endoribonuclease domain (Dziembowski et al., 2007; Lebreton et al., 2008; Lorentzen et al., 2008; Schaeffer et al., 2009; Schneider et al., 2007, 2009). In contrast, the human complex can associate with two different RNase II/R homologs, human (h)DIS3 or (h)DIS3L1, in the nucleus or cytoplasm, respectively (Staals et al., 2010; Tomecki et al., 2010). In the nucleus/nucleolus, the Ski2-like RNA helicase yMtr4/hMTR4 associates with the exosome cap and unwinds structured RNAs substrates directing them as single-stranded RNAs into the central channel and toward the yRrp44/hDIS3 active site, which is poised at the barrel exit (Bonneau et al., 2009; Jackson et al., 2010; Schneider & Tollervey, 2013; Schneider & Tollervey, 2014; Weick et al., 2018; Weick & Lima, 2021; Weir et al., 2010). Substrates can be directed from the channel to either the PIN domain or exoribonuclease active site of yRrp44/hDIS3 (Delan-Forino et al., 2017; Drazkowska et al., 2013; Han & van Hoof, 2016; Liu et al., 2014; Makino et al., 2013, 2015; Malet et al., 2010; Schneider et al., 2012), but substrates can also be cleaved by the PIN domain without entering the core complex.

Further catalytic activity is provided to the exosome by the RNase D-like 3′-5′ exoribonuclease yRrp6/hEXOSC10 and its cofactors yRrp47/hC1D and yMpp6/hMPP6 (Briggs et al., 1998; Falk et al., 2017; Milligan et al., 2008; Mitchell et al., 2003; Schilders et al., 2007; Schuch et al., 2014; Wasmuth et al., 2014, 2017; Weick et al., 2018). yRrp6/hEXOSC10 possess distributive 3′-5′ exoribonucleolytic activity employed to degrade substrates that do not pass through the channel of the complex (Das et al., 2021; Januszyk et al., 2011; Makino et al., 2015).

The exosome not only contributes to pre-rRNA processing, but also associates with a number of nuclear and cytoplasmic cofactors to mediate the quality control and degradation of various other transcripts (Sloan et al., 2012; Zinder & Lima, 2017).

2.2 | RNase MRP

RNase MRP is a multi-subunit RNP that is closely related to, and shares protein components with, the pre-tRNA processing ribozyme RNase P (Esakova et al., 2013; Esakova & Krasilnikov, 2010; Lan et al., 2020; Perederina et al., 2020; Walker & Engelke, 2006). Despite displaying weak sequence homology, the RNA components of RNase MRP and P fold into similar secondary structures, especially with regards to the region corresponding to the catalytic domain of RNase P, with many of the specific residues pinpointed as important for catalysis being conserved in RNase MRP. This is highly suggestive of a conserved ribozyme function, with the yNme1/hRMRP RNAs being the catalytic component of RNase MRP (Li et al., 2004; Walker & Engelke, 2006). RNase MRP is multifunctional as beside its role in pre-rRNA processing (see below), it also has mRNA targets and is involved in cyclin-dependent cell cycle regulation and cellular signaling (Chen et al., 2021; Gill et al., 2004; Mattijssen et al., 2011).

3 | 5′ ETS PROCESSING AND TURNOVER

In yeast, the 5′ ETS is removed in two steps via cleavages at sites A_0 and A_1, and in humans, in three steps via cleavages at A′, A0, and A1 (Figures 1 and 2a; Tomecki et al., 2017). Removal of the 5′ ETS is a critical early step in ribosome production and it has emerged that turnover of the excised pre-rRNA fragments is intertwined with pre-rRNA cleavage and particle biogenesis. Compositional and structural analyses have enabled a series of initial pre-ribosomal particles to be defined, based on their pre-rRNA composition: (i) the 5′ ETS RNP containing an unprocessed 5′ ETS, (ii) the pre-A_1/A1 particle in which cleavage at A_0/A0 has occurred, (iii) the pre-A_1/A1* particle where the 5′-A_0/A′-A0 fragment is degraded and the context for A_1/A1 processing is established, (iv) the post-A_1/A1 complex where A_1/A1 cleavage has taken place, and (v) various disassembly intermediates in which early assembly factors dissociate and pre-40S particles are formed (Vanden Broeck & Klinge, 2022).

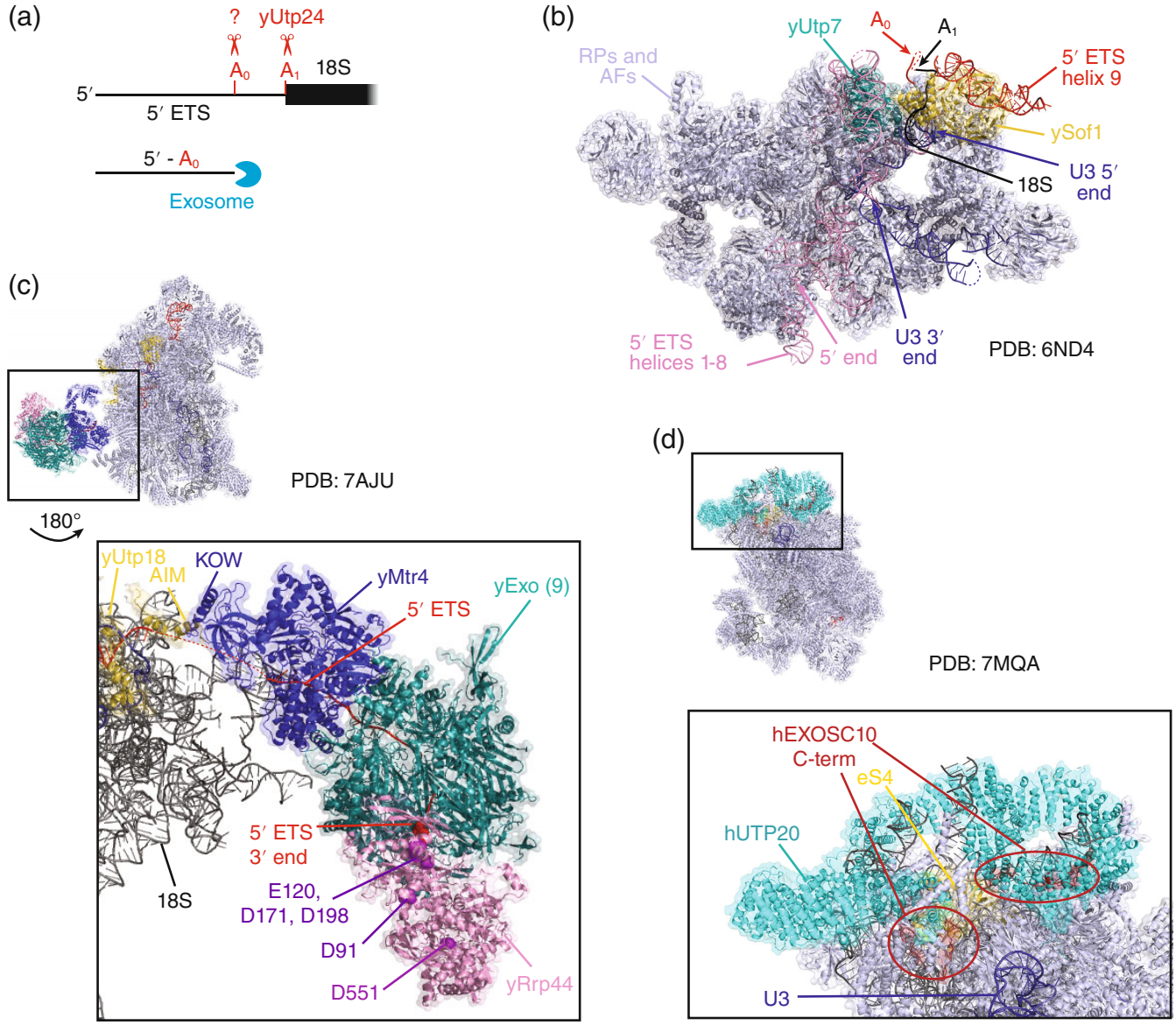

FIGURE 2 Processing and turnover of the 5′ ETS. (a) Schematic view of the yeast 5′ ETS. (b) The tertiary structure of a yeast 5′ ETS RNP is shown. PDB: 6ND4. Helices 1–8 of the 5′ ETS are shown in pink and helix 9 in red, while a 5′ fragment of the 18S rRNA is displayed in black and the U3 snoRNA in blue. The positions of the A_0 and A_1 pre-rRNA cleavage sites are indicated. A nonresolved section of the 5′ ETS, connecting sites A_0 and A_1, is indicated by a red dotted line. ySof1 and yUtp7 are shown in cartoon view with a transparent surface in yellow and teal, respectively and all other proteins present in the complex are shown in blue-white. (c) The structure of a yeast post-A_1 particle associated with the exosome is shown. PDB: 7AJU. Key residues in yRrp44 (pink) required for catalysis are highlighted (PIN—D91, E120, D171, D198 and EXO—D551) and the arch-interacting motif (AIM) of yUtp18 (yellow) and Kyrpides–Ouzounis–Woese (KOW) domain of yMtr4 (blue) that mediate contacts between the core exosome (yExo 9, teal) and the SSU processome are indicated. Nonresolved sections of the 5′ ETS (red) are indicated by a dotted line. (d) Structure of a human post-A1 particle bound by hEXOSC10 (red) is shown. PDB: 7MQA. hUTP20 and eS4 are shown in cartoon mode with transparent surfaces in cyan and yellow, respectively. Contacts between hEXOSC10 and the SSU processome containing the U3 snoRNA (blue) are circled.

3.1 | Cleavage at site A_0/A0

Visualization of a 5′ ETS RNP from yeast (Hunziker et al., 2019) revealed that helices 7–9 of the 5′ ETS, which contain the A_0 cleavage site, lie in a groove between the noncatalytic early ribosome assembly factors ySof1 and yUtp7 (Figure 2b). In this particle, the A_0 site is relatively exposed and not directly contacted by any protein, implying that conformational rearrangements are likely required to bring the cleavage site into contact with the appropriate

ribonuclease and/or that the responsible ribonuclease associates with such particles weakly or transiently and is lost during complex isolation.

The A_0/A0 endoribonuclease remains elusive. The PIN domain protein yUtp23/hUTP23 was long speculated to perform this cleavage and although crosslinking mass spectrometry confirmed its association with the yeast 5′ ETS RNP complex (Chaker-Margot et al., 2015; Hoareau-Aveilla et al., 2012; Wells et al., 2017; Zhang et al., 2016), the degenerate nature of the PIN domain in yUtp23 (with only two of the four possible active site amino acids present, which can be mutated without phenotype) indicates that it is not the A_0 endoribonuclease (Bleichert et al., 2006; Lu et al., 2013; Wells et al., 2017).

An intact PIN domain in hUTP23, which contains three of the four possible active site residues, is, however, necessary for processing at site A0 (Wells et al., 2017). Structural analyses of hUTP23-containing 5′ ETS RNP particles may therefore shed light on how site A0 is cleaved in human cells.

3.2 | Exosome-mediated turnover of the 5′ ETS

Excitingly, recent structural snapshots of pre-A_1/A1 particles from a eukaryotic thermophile, yeast and human cells have revealed the association of the RNA exosome with these complexes to form processing competent pre-A_1/A1* particles (Chaker-Margot et al., 2017; Du et al., 2020; Kornprobst et al., 2016; Lau et al., 2021; Singh et al., 2021; Sun et al., 2017). Release of the early assembly factor yLcp5 in yeast or hNGDN in human cells, as well as remodeling of yUtp20/hUTP20 and eS4 in yeast and humans, allow recruitment of the RNA exosome. On the one hand, the exosome docks onto pre-A_1/A1 particles via the arch-interacting motifs (AIMs) of the SSU processome component yUtp18/hTDIF2, which mediates contacts with the Kyrpides–Ouzounis–Woese (KOW) domain of the arch region of the exosome-associated RNA helicase yMtr4/hMTR4 (Figure 2c) (Du et al., 2020; Lau et al., 2021; Thoms et al., 2015). On the other hand, the C-terminal "lasso" region of yRrp6/hEXOSC10 makes contact with yUtp20/hUTP20, sensing the conformation of the yUtp20/hUTP20-eS4 surface (Figure 2d) (Singh et al., 2021). These two specific contacts that depend on the availability and specific conformations of the interaction sites ensure accurate positioning of the exosome and its recruitment only to sufficiently mature pre-ribosomal particles in which the key recognition features are correctly assembled.

As anticipated, the structural analyses reveal the exosome to be poised in the vicinity of the A_0/A0 cleavage site, close to the base of the 5′ ETS helices 9-9′ (Lau et al., 2021). Importantly, the open conformation of yMtr4/hMTR4 upon pre-ribosome binding situates the 3′ end of the 5′ ETS-A_0/A0 fragment such that it can traverse the RecA-like domains of the helicase core and be channeled toward the ribonuclease subunits of the exosome (Figure 2c). Visualization of the 5′ ETS-A_0 fragment in progressively maturing particles supports the exosome-mediated turnover of the excised spacer fragment as progressive rearrangement and shortening is observed (Du et al., 2020; Lau et al., 2021).

Unwinding of helices 9, 8, and 7 of the 5′ ETS-A_0 fragment occurs without significant effects on particle structure, but ongoing processing through helix 6 leads to displacement of specific assembly factors and other conformational rearrangements, priming the particle for A_1 cleavage (see below). Notably, the pre-ribosomal contact sites of the exosome maintain similar structures even after A_1 cleavage has occurred. This implies that partial degradation of the 5′ ETS-A_0 fragment is sufficient to license A_1 cleavage and separation of the remaining 5′ ETS sequence from the mature 18S rRNA 5′ end to establish the primordial pre-40S particle. Complete degradation of the 5′ ETS-A_0 fragment by the RNA exosome occurs after A_1 cleavage and induces further displacement of assembly factors binding to the 5′ ETS, for example, yUtp-A/hUTP-A, and leads, ultimately, to disassembly of the SSU processome (Cheng et al., 2020).

Biochemical experiments demonstrate that the A_0-A_1/A0-A1 fragment released by cleavage at site A_1/A1 accumulates in cells lacking yRat1/hXRN2 (Petfalski et al., 1998; Sloan et al., 2014), but thus far, these 5′-3′ exoribonucleases have not been captured on disassembling SSU processomes. It is likely that this assembly stage has simply not yet been captured due to its transient nature, but it is also possible that degradation of the A_0-A_1/A0-A1 fragment occurs outside the context of the pre-ribosome when most of the bound assembly factors have dissociated.

3.3 | A_1/A1 cleavage by yUtp24/hUTP24

Degradation of the 5′ ETS-A_0/A0 fragment and pre-rRNA folding chaperoned by the U3 small nucleolar RNP are intimately linked with cleavage at site A_1/A1 that forms the mature 5′ end of the 18S rRNA and which is carried out by the PIN domain endoribonuclease yUtp24/hUTP24 (Tomecki et al., 2015; Wells et al., 2016).

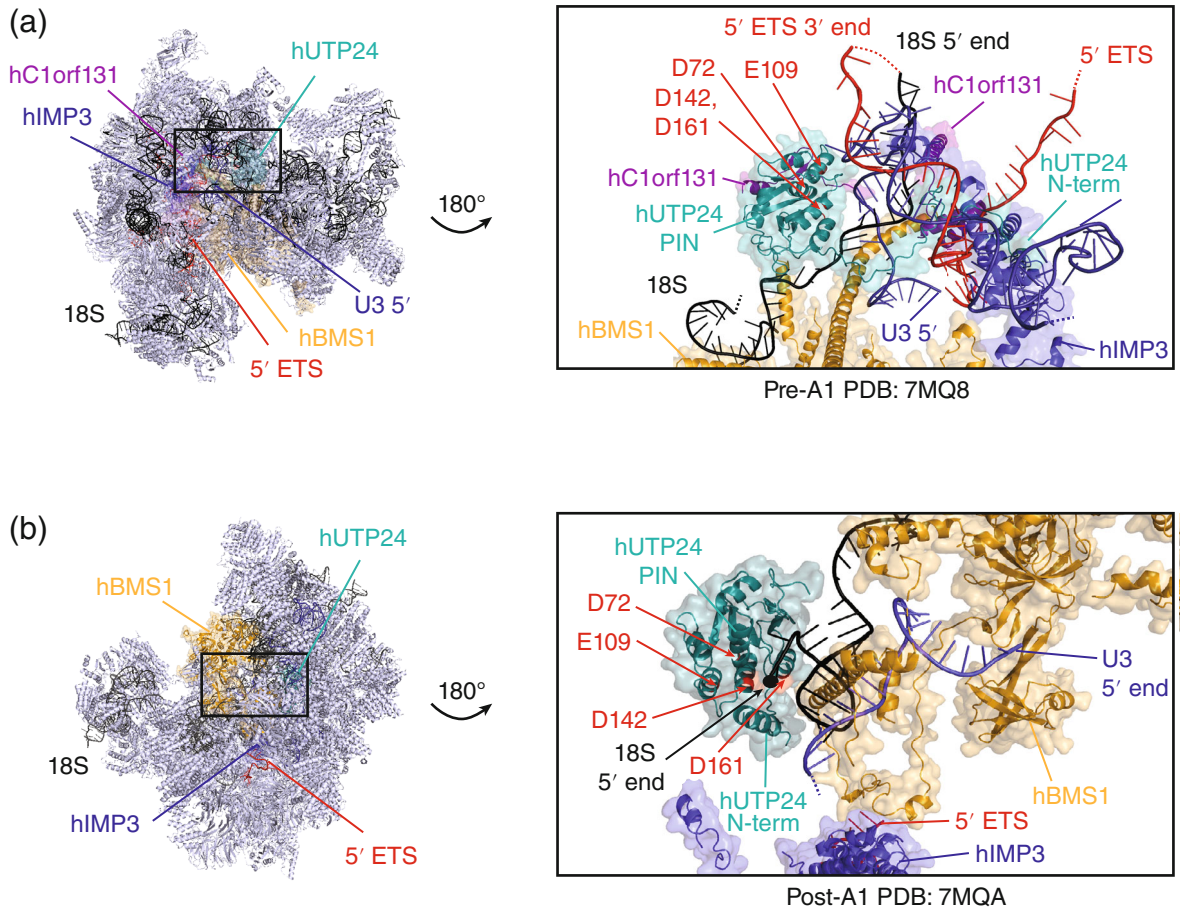

FIGURE 3 Conformations of hUTP24 in pre- and post-A1 particles. (a) Tertiary structure of a human pre-A1 particle (PDB: 7MQ8) in which hUTP24 (teal) is in an extended conformation where the PIN domain (D72, E109, D142, D161 catalytic residues marked in red) is sterically blocked by the presence of hC1orf131 (purple). The 5′ end of the 18S rRNA (black) (site A1) is held away from hUTP24 by hBMS1 (yellow) and hIMP3 (blue). A nonresolved section of the 5′ ETS, connecting sites A0 and A1, is indicated by a red dotted line. An overview (left) and a magnified view (right) are shown as mirror images to maximize visibility of features of interest. (b) Tertiary structure of a human post-A1 particle (PDB: 7MQA) where hC1orf131 has dissociated and hBMS1 (yellow), the U3 snoRNA (blue) and hIMP3 (blue) are rearranged to bring the 5′ end of the 18S rRNA (black) close to the hUTP24 (teal) PIN domain. hUTP24 has also undergone structural rearrangements such that the N-terminal region forms a lid facilitating capture/cleavage of site A1. An overview (left) and a magnified view (right) are shown as mirror images to maximize visibility of features of interest.

In pre-A1 particles, the 3′ end of the 5′ ETS and 5′ end of the 18S rRNA are held at a distance from hUTP24 through the specific arrangement of the assembly factors hBMS1, hIMP3, hIMP4, hNOP14, and hC1orf131 (Singh et al., 2021). hUTP24 is trapped between hIMP3, hPWP2, and hWDR46, and hC1orf131 physically obstructs interactions between hUTP24 and the pre-rRNA (Figure 3a). Conformational changes arising from the exosome-mediated degradation of the 5′ ETS trigger dissociation of hC1orf131 and placement of the 5′ end of the 18S rRNA into the active site of the endoribonuclease as well as rearrangement of the N-terminal region of hUTP24 to stabilize interactions with the pre-rRNA allowing cleavage (Figure 3b).

Likewise, the yeast homolog of hC1orf131, yFaf1, is positioned between the 5′ ETS and the Box A duplex of the U3 snoRNA, near yImp3 and yImp4, and a linker of yFaf1 occludes access to the active site of yUtp24 in the pre-A_1 particle (Barandun et al., 2017). Unwinding and removal of 5′ ETS helix 6 then eliminates the binding sites for yFaf1 (and yKrr1), liberating the previously constrained Box A and exposing yUtp24 for cleavage (Cheng et al., 2020; Du et al., 2020). In addition, a "ring opening step," pulling parts of the 5′ ETS out of a clamp between yUtp7/hUTP7 and yPwp2/hPWP2, is required for A_1/A1 cleavage to proceed in both yeast and human cells (Cheng et al., 2020; Du et al., 2020; Lau et al., 2021; Singh et al., 2021).

While the uncleaved A_1 site is ~50 Å away from the catalytic center of yUtp24 in the pre-A_1 state complex, the formation of a short RNA stem-loop (h1) at the 5′ end of the mature 18S rRNA in the post-A_1 state suggests that A_1

cleavage is initiated by relocation of the pre-18S rRNA substrate rather than by movement of yUtp24 toward the cleavage site (Cheng et al., 2020). In this context, it is important to note that yUtp24/hUTP24 remains associated with post-A_1/A1 complexes and various disassembly intermediates, including the yeast Dis-C complex which predominantly contains the 20S intermediate that has undergone cleavage at site A_2 in ITS1. While yUtp24 appears to be dislodged in Dis-B complexes after A_1 cleavage, it is still tethered to the pre-ribosome potentially allowing it to access the A_2 cleavage site in ITS1 (Cheng et al., 2020). These data support the longstanding idea that processing at sites A_1/A1 at the 5′ end of 18S and A_2/2a(E) in ITS1 is coupled and performed by the same enzyme (Bleichert et al., 2006; Wells et al., 2016).

Furthermore, yUtp24 also appears to be critical in the elimination of unprocessed particles and in consequence, recycling of assembly factors, for example when early cleavages within the SSU processome are impaired. In this instance, yUtp24 turns from a processing enzyme into a bona fide quality control factor that cleaves pre-18S intermediates within the mature sequence of the 18S rRNA to initiate turnover of the aberrant pre-40S pre-ribosomal particles (Choque et al., 2018).

4 | ITS1 PROCESSING

In budding yeast, the major ITS1 cleavage occurs at the proximal site A_2, separating SSU and LSU pre-rRNA processing pathways. Cleavage at the distal ITS1 site, A_3, enables LSU maturation via 5′-3′ exoribonucleolytic processing to produce the $5.8S_S$ isoform and disruption of this cleavage event leads to an alternative pre-rRNA processing pathway involving another endoribonucleolytic cleavage that generates $5.8S_L$ (Henras et al., 2015). Cleavage at site A_3, is not required for normal SSU maturation, which is concluded by a single endoribonucleolytic cleavage at site D to generate the 3′ end of the mature 18S rRNA. In contrast, the major pre-rRNA processing pathway in human cells appears to favor a primary cleavage at the distal ITS1 site, 2, followed by 3′-5′ exoribonucleolytic processing from site 2 and final endoribonucleolytic cleavages at sites 2a/E and 3 to complete 18S 3′ end maturation (Henras et al., 2015; Mullineux & Lafontaine, 2012; Tomecki et al., 2017). While cleavage at the proximal ITS1 site has not been captured yet, cleavage at site A_3 in yeast has been visualized (Lan et al., 2020; Perederina et al., 2020) and structures of late pre-40S particles from yeast and human cells give new insights into the final steps of 18S rRNA 3′ end maturation (Vanden Broeck & Klinge, 2022).

4.1 | Processing at A_2/2a(E)

Both yUtp24/hUTP24 and yRcl1 have been postulated to be the enzyme responsible for the proximal cleavage site in ITS1, A_2/2a(E), which is the main cleavage event that separates the assembly pathways of the small and large ribosomal subunits in yeast (Horn et al., 2011; Wells et al., 2016). Notably, yUtp24/hUTP24 is still detected in post-A_1/A1 particles (see above), implying that A_1/A1 cleavage and ribonuclease dissociation are not directly linked. It is anticipated therefore that through additional particle rearrangements upon release of the U3 snoRNA, the active site of yUtp24/hUTP24 (or yRcl1/hRCL1) may be brought into contact with the A_2/2a(E) cleavage site. Although a plethora of structures of later pre-40S particles containing the 20S (yeast)/18SE (human) pre-rRNAs are available, none containing ITS1 with an uncleaved site A_2/2a(E) have been resolved, leaving this early stage of pre-40S maturation something of a "black box," and knowledge on how site A_2/2a(E) cleavage is achieved and regulated is limited.

4.2 | RNase MRP-mediated cleavage of site A_3

A conserved machinery, RNase MRP, is responsible for site A_3/2 cleavage, which provides entry points for exoribonucleolytic processing in yeast and humans. RNase MRP is one of the few ribonucleolytic ribozymes in eukaryotes, raising the question why RNA-catalyzed pre-rRNA cleavage is preferred and has been maintained throughout evolution. While RNase MRP is yet to be visualized on pre-ribosomal particles, recent cryo-EM structures of yeast RNase MRP, one of them in complex with its ITS1 target site, have provided important insights into how this holoenzyme recognizes its specific target site within such complexes (Lan et al., 2020; Perederina et al., 2020).

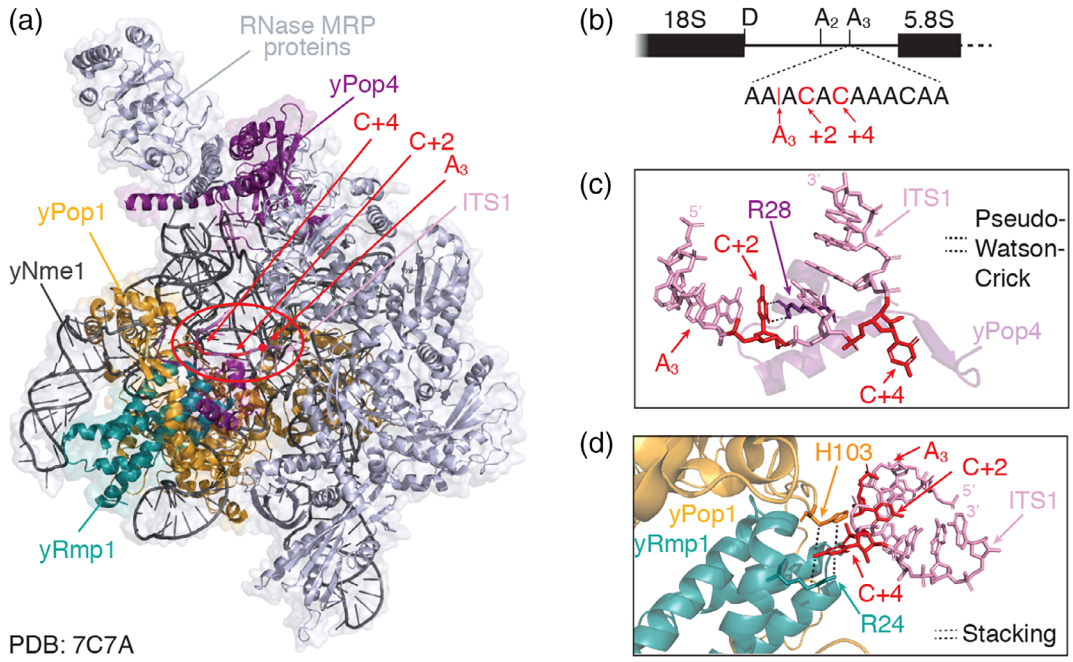

FIGURE 4 RNase MRP-mediated cleavage of site A_3 in ITS1. (a) The tertiary structure of yeast RNase MRP with a 12 nucleotide fragment of the ITS1 RNA encompassing the A_3 cleavage site and key downstream features is shown. PDB: 7C7A. The RNA component (yNme1) of RNase MRP is shown in gray and the ITS1 RNA fragment is red with the A_3 cleavage site indicated. yPop4, yPop1, and yRmp1, which contain key target recognition elements, are shown in purple, yellow and teal, respectively, while all other protein components of RNase MRP are depicted in blue-white. Cartoon mode is used as well as a transparent surface view. (b) Schematic view of the yeast ITS1 with the proximal and distal cleavage sites marked. The sequence context of the A_3 cleavage site within the ITS1 fragment visualized in (a) is shown. (c) Magnified view of Pseudo–Watson–Crick base-pairing between R28 of yPop4 (purple) and the cytidine two nucleotides downstream of the A_3 cleavage site (C + 2). (d) Magnified view of stacking interactions between H103 of yPop1 (yellow), R24 of yRmp1 (teal) and the cytidine four nucleotides downstream of the A_3 cleavage site (C + 4).

The overall architecture of yeast RNase MRP (Figure 4a) is similar to its well-known counterpart RNase P, and both complexes appear to employ common mechanisms to nonspecifically bind 5′ of the cleavage site, for example base stacking between the substrate and the catalytic RNAs or electrostatic interactions of the substrate with shared protein components, like yPop5. However, due to unique auxiliary elements in the RNase MRP catalytic RNA yNme1, together with RNA-driven remodeling of several RNase MRP proteins, the substrate binding pockets of RNase MRP and RNase P are substantially different (Perederina et al., 2020). As a consequence, RNase MRP has acquired the ability to recognize a weak sequence motif, whereas RNase P solely relies on RNA secondary structural elements to target its pre-tRNA substrates (Lan et al., 2020).

The ITS1 region surrounding the A_3 cleavage site forms an extensive interface with the RNA component of RNase MRP with numerous intermolecular base stacking events stabilizing substrate interactions. While, like in RNase P, these connections are predominantly formed with the ITS1 backbone rendering them nonsequence specific, substrate specificity is endowed by the particular arrangement of protein components of RNase MRP that recognize two cytidines located at positions two and four downstream of the cleavage site (Figure 4b). First, arginine 28 (R28) of yPop4 forms "Pseudo-Watson-Crick" base pairs with the cytidine two nucleotides downstream of the RNase MRP target site by coordinating two electrostatic interactions (Figure 4c). In contrast, the cytidine four nucleotides downstream of the A_3 cleavage site is flipped out and forms stacking interactions with arginine 24 (R24) and histidine 103 (H103) of yRmp1 and yPop1, respectively (Figure 4d). The nature of the interactions of these two ITS1 nucleotides strongly favors the presence of cytidines at these positions as well as the presence of purines at positions one and three downstream of the cleavage site. The identification of this sequence recognition motif rationalizes how the specific cleavage site of RNase MRP is defined within the local ITS1 region, but how RNase MRP is recruited to pre-60S particles and how the timing of this cleavage event is regulated, remain to be resolved.

In line with the weak recognition motif, it has been suggested that RNase MRP may mediate additional, earlier pre-rRNA cleavage events alongside processing its major target site at A_3/2. First, depletion of RNase MRP leads to accumulation of the 35S and 41S pre-rRNAs in yeast and humans, respectively, and in vitro cleavage of ITS1 substrates with RNase MRP isolated from human cells has led to the formation of additional products (Goldfarb & Cech, 2017; Lindahl et al., 2009). Moreover, RNase MRP-dependent changes in the ratio of yeast 5.8S rRNA isoforms, traditionally attributed to the use or bypass of A_3 cleavage, were found to also occur when the A_3 cleavage site is deleted (Li et al., 2021).

4.3 | 18S 3′ end maturation

In both yeast and human cells, cleavage at the 3′ end of the 18S rRNA at site D/3 by yNob1/hNOB1 is one of the final maturation events during 40S biogenesis that generates translation-competent subunits (Fatica et al., 2003, 2004; Pertschy et al., 2009; Preti et al., 2013; Sloan et al., 2013). In yeast, this important cleavage event is coupled to formation of 80S-like particles and a translation-like cycle that is thought to serve a proof-reading function (Belhabich-Baumas et al., 2017; Lebaron et al., 2012; Rai et al., 2021; Strunk et al., 2012).

Interestingly, yNob1/hNOB1 joins pre-40S particles already in the nucleolus but its catalytic action is tightly regulated until other maturation events have been successfully completed and the pre-rRNA is licensed for cleavage. In pre-D/3 complexes, the partner of yNob1/hNOB1, yPno1/hPNO1, which forms extensive interactions with the C-terminal region of yNob1/hNOB1 via a groove between its tandem KH domains, plays a pivotal role in holding helix 28 and helices 44/45 of the 18S pre-rRNA in immature conformations. In addition, the KH domains of yPno1/hPNO1 and a patch of positively charged residues within the C-terminal region of yNob1/hNOB1 directly bind the 3′ end of the 18S rRNA and the 5′ end of ITS1 (Ameismeier et al., 2018; Ameismeier et al., 2020; Heuer et al., 2017; Scaiola et al., 2018).

These protein–protein and protein-RNA interactions hold the site D/3 cleavage site at a considerable distance (~30 Å) from the active site of yNob1/hNOB1, thus preventing cleavage from taking place (Figure 5a). Export of late pre-40S particles to the cytoplasm and further structural remodeling in the cytoplasm is accompanied by the progressive shedding of assembly factors (Cerezo et al., 2019; Hector et al., 2014; Mitterer et al., 2019; Shayan et al., 2020). Release of yTsr1/hTSR1 and yLtv1/hLTV1 initiates pre-rRNA rearrangements that bring helices 28, 44, and 45 of the 18S rRNA into their final orientations enabling recruitment of yRio1/hRIOK1. The overlapping positions of the flexible loop

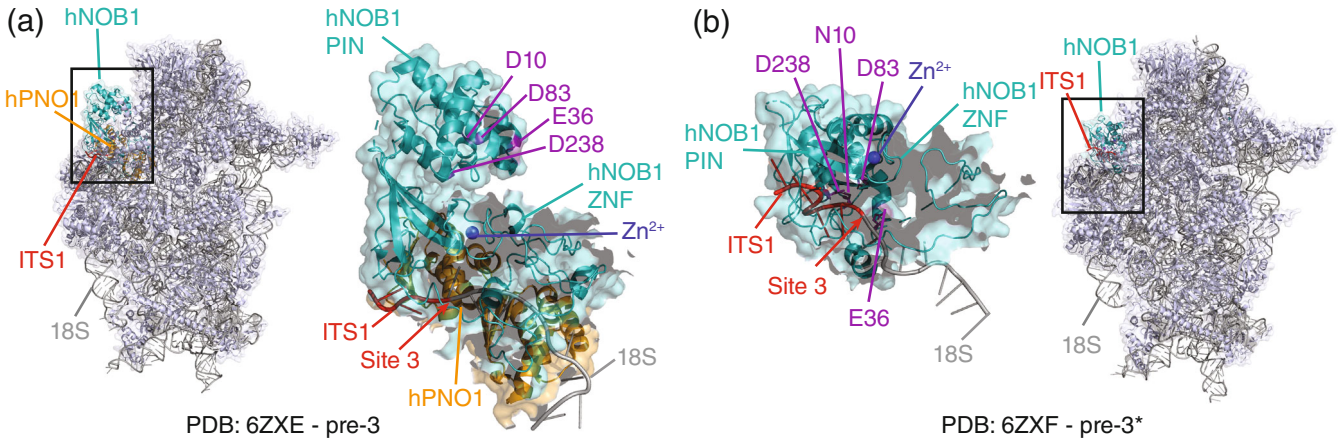

FIGURE 5 Conformational rearrangements allowing cleavage of the 3′ end of the 18S rRNA by hNOB1. (a) Tertiary structure of a human cytoplasmic pre-SSU particle (PDB: 6ZXE), in which hPNO1 (yellow) sterically occludes the 18S rRNA 3′ end (gray)-ITS1 (red) junction (site 3). hNOB1 (teal) is bound in an open conformation in which the zinc finger domain (ZNF) is proximal to the 18S rRNA, but the catalytic PIN domain (D10, E36, D83, and D238 catalytic residues marked in purple) is distant. By analogy to nomenclature adopted for structural snapshots of particles, this state is termed pre-3. An overview (left) and a magnified view of hNOB1 and hPNO1 (right) are shown. (b) Tertiary structure of a human cytoplasmic pre-SSU particle containing catalytically inactive hNOB1 (D10N; PDB: 6ZXF), where hNOB1 (teal) has undergone a substantial rearrangement such that the PIN domain (N10, E36, D83, D238 catalytic residues marked in purple) contacts the 18S rRNA 3′ end (gray)-ITS1 (red) junction (site 3). By analogy to nomenclature adopted for structural snapshots of particles, this state is termed pre-3*. An overview (right) and a magnified view of hNOB1 on its pre-rRNA substrate (left) are shown.

of yRio1/hRIOK1 and the C-terminal region of yPno1/hPNO1 indicate that these events trigger the release of yPno1/hPNO1, which is also supported by biochemical evidence (Ameismeier et al., 2020; Plassart et al., 2021; Turowski et al., 2014).

Pre-40S particles lacking yPno1/hPNO1, but containing yNob1/hNOB1, have only been captured by impeding the catalytic activity of yNob1/hNOB1, suggesting that upon yPno1/hPNO1 dissociation, yNob1/hNOB1 rapidly exerts site D/3 cleavage and dissociates. Release of hPNO1 enables the catalytically inactive hNOB1 (D10N) mutant to dramatically change its conformation such that the PIN domain rotates relative to its zinc-finger (ZNF) domain that mediates contacts with the 18S pre-rRNA. Concurrently, the 18S rRNA 3′ end-ITS1 junction is repositioned so that site 3 lies within the catalytic site of the hNOB1-D10N PIN domain (Figure 5b) (Ameismeier et al., 2018, 2020). In its active conformation, yNob1 has been shown to form extensive interactions with nucleotides at the 5′ end of ITS1 leading to the suggestion that yNob1/hNOB1 dissociates from pre-40S complexes together with the cleaved pre-rRNA fragment (Lamanna & Karbstein, 2009; Turowski et al., 2014).

4.4 | ITS2 processing

Removal of ITS2 that separates the 5.8S and 25S/28S rRNAs is initiated by a central endoribonucleolytic cleavage at site C_2/4. This cleavage provides an entry point for exoribonucleolytic processing enzymes to generate the mature 5′ and 3′ ends of the 25S/28S and 5.8S rRNAs, respectively (Figure 6a) (Bohnsack & Bohnsack, 2019; Tomecki et al., 2017).

4.5 | Endoribonucleolytic cleavage of C_2/4 and maturation of the 5′ end of the 25S rRNA

In yeast, C_2 cleavage and maturation of the 5′ end of the 25S rRNA take place via a multi-step process involving the HEPN domain-containing endoribonuclease yLas1, the polynucleotide kinase yGrc3, the 5′-3′ exoribonuclease yRat1 and its cofactor yRai1 as well as yDxo1 (Castle et al., 2010, 2013; Fromm et al., 2017; Gasse et al., 2015; Hurtig & van Hoof, 2022; Pillon et al., 2017). These different enzymes work in concert to generate the mature 5′ end of the 25S rRNA and provide a substrate for processing to generate the 3′ end of the 5.8S rRNA. All these proteins have human homologs, and lack of hLAS1L impairs ITS2 processing and hXRN2 is known to be involved in forming the 5′ end of the 28S rRNA suggesting that the complex and processing mechanism are likely conserved to humans (Castle et al., 2012; Preti et al., 2013; Schillewaert et al., 2012; Sloan et al., 2013; Tafforeau et al., 2013).

A recent cryo-EM structure of the Las1-Grc3 module from *Chaetomium thermophilum* provides insights into how a complex, also referred to as "RNase PNK," recognizes and processes its ITS2 target (Figure 6b; Pillon et al., 2019). Similar to other HEPN nucleases, dimerization of cLas1 is necessary for catalytic activity and in this case, each cLas1 molecule is flanked by a cGrc3 molecule giving rise to an RNase PNK tetramer with a butterfly-like architecture in which the cLas1 dimer forms the body and the cGrc3's are the wings. Although present, RNA was not visualized in the structural analyses, likely due to efficient cleavage and dissociation. Positively charged RNA-binding grooves that can accommodate single- or double-stranded RNAs lie between the body and wing structures (Figure 6b), but only one RNA is bound asymmetrically at a given time. The RNA substrate is directed toward the ribonuclease active site in the "head" region of cLas1 and a noncatalytic, evolutionarily conserved histidine residue (H142) functions as a switch, regulating ribonuclease activity. After cleavage at the C_2 site, which generates a 5.8S rRNA precursor (7S) with a 2′, 3′ cyclic phosphate at the 3′ end and a 25S rRNA precursor (26S) with a 5′ hydroxyl group (Figure 6c; Gasse et al., 2015), the RNA is directed toward one of the distal kinase active sites in the cGrc3 wing. The precise route of the RNA remains unknown; either it remains in the same RNA-binding channel and rotates toward the kinase active site on the adjacent wing, or it traverses the complex to reach the active site on the other wing. ATP-dependent mono-phosphorylation of the 26S pre-rRNA 5′ end then renders it an appropriate substrate of 5′-3′ exoribonucleolytic trimming by yRat1 (Figure 6c). In contrast to related endoribonucleases, the active site of yRat1 resembles a cleft, enabling it to function exclusively as an exoribonuclease (Xiang et al., 2009). The catalytic center of Xrn2 from *C. thermophilum* is dynamic and adopts an active conformation upon binding RNA and magnesium (Overbeck et al., 2022). Furthermore, yRat1 activity is stimulated by the presence of yRai1, a cofactor protein that functions by stabilizing the exoribonuclease rather than directly influencing the conformation of the active site (Xiang et al., 2009). Structural analysis of the related 5′-3′ exoribonuclease hXRN1 together with an RNA substrate rationalizes the preference of yRat1 for RNAs with a 5′ phosphate; the 5′ nucleotide of the substrate is stacked between aromatic side chains and the negatively charged

phosphate group is embedded within a highly basic pocket characteristic of XRN family ribonucleases (Jinek et al., 2011). After removal of the majority of the 3′ ITS2 sequence by the processive activity of yRat1, final maturation of the 5′ end of the 25S rRNA is accomplished by the distributive exoribonuclease yDxo1 (Hurtig & van Hoof, 2022). The sequential action of a processive and a distributive exoribonuclease draws parallels to the mechanism of substrate processing by the exosome-associated yRrp44/hDIS3 and yRrp6/hEXOSC10 ribonucleases, suggesting that it may be a common mechanism for the precise generation of mature RNA ends.

The functions of yLas1-yGrc3 and yRat1-yRai1 are closely coordinated and the four proteins can be efficiently co-enriched from yeast, but it remains unknown if they directly interact, and how the RNA substrate is passed from the

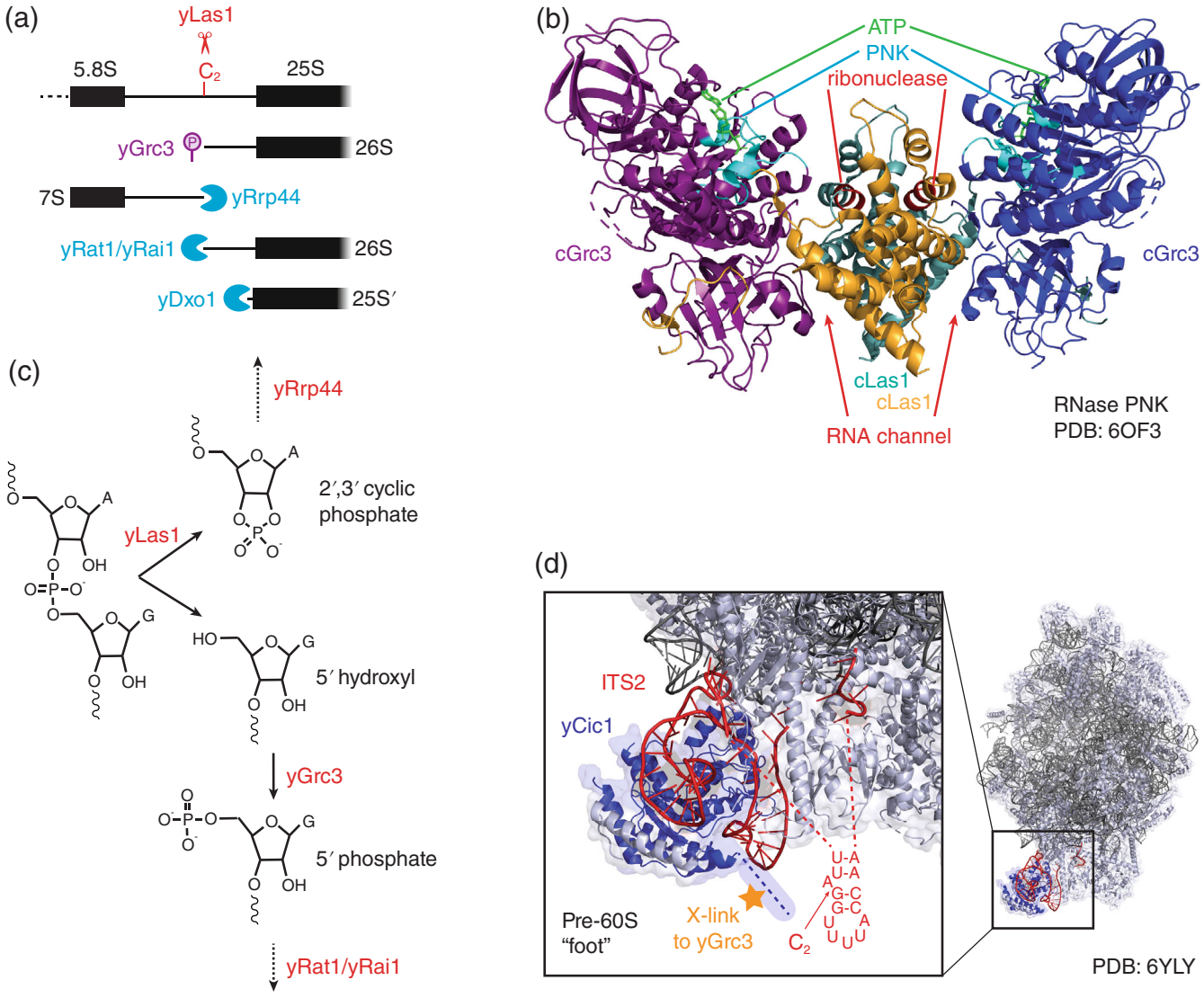

FIGURE 6 Processing of ITS2 by the RNase PNK complex. (a) Schematic view of yeast ITS2 processing by the endoribonuclease-kinase complex yLas1-yGrc3 to generate the 7S and 26S pre-rRNA intermediates that are further processed by yRrp44, yRat1/yRai1 and yDxo1, respectively. (b) Tertiary structure of the RNase PNK complex from *Chaetomium thermophilum* composed of two cLas1 (light orange and teal) and two cGrc3 (purple and dark blue) molecules joined by cLas1 dimerization (PDB: 6OF3). The catalytic sites of cLas1 (ribonuclease) are marked in red and the kinase sites of cGrc3 (PNK) are highlighted in cyan. Bound ATP is shown in green and the mutually exclusive RNA-binding channels are indicated. (c) Chemical structure of the yeast C_2 cleavage site and the nucleotide derivatives. Yeast ribonucleases and the kinase involved are marked in red. (d) Cryo-EM structure of a yeast pre-LSU particle purified via yNop53 (PDB: 6YLY) is shown with the 25S, 5.8S, and 5S rRNA in dark gray and ITS2 fragments in red. LSU RPs and assembly factors are shown in cartoon mode with a transparent surface in blue-white except yCic1 in dark blue. In the magnified view, the nonvisualized region of ITS2 containing the C_2 cleavage site is shown as a dotted red line with key nucleotides indicated. The nonresolved C-terminal region of yCic1 containing the amino acids crosslinked to yGrc3 (orange star) is shown as a blue dotted line within a transparent bubble.

active site of yGrc3 to yRat1 (Gasse et al., 2015). yLas1, yGrc3, yRat1, and yRai1 have not yet been visualized on pre-60S particles purified from yeast, however, structural views of ITS2-containing pre-60S complexes demonstrate that ITS2, together with associated factors yCic1, yNop15, yRlp7, yNop7, and yNop53, constitutes a prominent "foot" structure on the base of these particles (Fromm et al., 2017). A recent crosslinking mass spectrometry approach applied to a spectrum of pre-60S particles (Sailer et al., 2022) revealed that yGrc3, likely in complex with yLas1, is co-recruited to nucleoplasmic complexes with the yRea1 AAA-ATPase-yRix1 complex and that yGrc3 directly interacts with the C-terminal region of yCic1, an assembly factor that binds ITS2 and is located in the foot structure (Figure 6d; Granneman et al., 2011; Kater et al., 2020; Wu et al., 2017). This provides evidence of the physical proximity of yLas1-yGrc3 with its substrate RNA in the context of a yeast pre-60S particle. Furthermore, yRix1-yRea1-containing pre-60S particles both with and without an ITS2-containing foot structure have been observed (Kater et al., 2020), consistent with the action of yLas1-yGrc3-yRat1-yRai1 in ITS2 processing and degradation in these complexes.

4.6 | Maturation of the 3′ end of the 5.8S rRNA

Following site C_2/4 cleavage by yLas1/hLAS1L, formation of the mature 3′ end of the 5.8S rRNA is a multistep process spanning the nucleoplasm and cytosol. Biochemical experiments have demonstrated the requirement of the RNA exosome and yRrp44/hDIS3 for generating the 5.8S + 30/5.8S + 40 intermediates that are then further processed to 6S by yRrp6/hEXOSC10 (Figure 7a; Briggs et al., 1998; Davidson et al., 2019; Lebreton et al., 2008; Schaeffer et al., 2009; Schneider et al., 2009; Tafforeau et al., 2013; Tomecki et al., 2010, 2017). Finally, in the cytosol, the remaining nucleotides of ITS2 are removed by yNgl2 in yeast or mERI1 in mammalian cells (Ansel et al., 2008; Faber et al., 2002; Pirouz et al., 2019; Thomson & Tollervey, 2010).

Excitingly, the nucleoplasmic steps in this process have recently been illuminated by a structure of a late yeast pre-60S particle associated with the exosome (Figure 7b). To capture these snapshots, processing of ITS2 was stalled by expression of a catalytically inactive version of yRrp6, leading to a pre-60S particle associated with the complete exosome complex and the 5.8S + 30 pre-rRNA. Compared to 7S pre-rRNA-containing particles, these structures reveal a substantially reorganized "foot" region, consistent with the observation that 5′-3′ processing of the 26S pre-rRNA to 25S′ by yRat1-yRai occurs prior to 7S processing and that, in the captured particles, 7S is in the process of being degraded (Fromm et al., 2017).

Similar to the association of the exosome with pre-A_1 particles (see above), yMtr4 serves as a key contact point anchoring the exosome to its substrate complex (Schuller et al., 2018). The yMtr4 KOW domain within the arch contacts helices 15–16 in domain I of the 25S RNA (Figure 7c) and the AIM of yNop53, a 5.8S pre-rRNA binding protein previously characterized as an adaptor for the exosome (Lingaraju, Johnsen, et al., 2019; Schuller et al., 2018; Thoms et al., 2015; Thomson & Tollervey, 2005). yMtr4 also contacts domain V of the 25S rRNA, filling space previously occupied by the ITS2 region that has been trimmed and now lies within the central channel of the exosome. The 2′, 3′-cyclic phosphate left on the 3′ end of 7S by yLas1 likely cannot be accommodated in the yRrp6 active site (Lingaraju, Schuller, et al., 2019), ensuring that the RNA substrate is directed through the channel toward yRrp44, which is able to process RNAs with such ends (Zinder et al., 2016).

Reconstitution of ITS2 processing has demonstrated the requirement of both the exoribonuclease and PIN domains of yRrp44 for 7S processing. The path through the central channel of the yeast exosome also containing yMtr4 in a relaxed conformation shields approximately 40 nucleotides, but it is proposed that compaction of the yMtr4-associated exosome complex due to the force exerted by the large pre-60S complex allows further trimming to within 30 nucleotides of the 3′ end of the 5.8S rRNA. It is then proposed that the pressure leads to expulsion of the 3′ end of the 5.8S + 30 pre-rRNA, carrying a 3′ hydroxyl group, from the exosome core channel. In agreement with in vivo crosslinking data following the path of substrates through the exosome (Delan-Forino et al., 2017; Schneider et al., 2012; Schneider & Tollervey, 2014), this would enable further processing by yRrp6 until the 6S pre-RNA containing approximately six nucleotides of ITS2 is formed, with the final ITS2 nucleotides likely protected from processing within the yMtr4 helicase that sterically blocks yRrp6. This model implies that the exosome complex does not automatically dissociate when processing of its substrate is complete, leaving open the question of what triggers release of the exosome prior to nuclear export of the pre-60S particles.

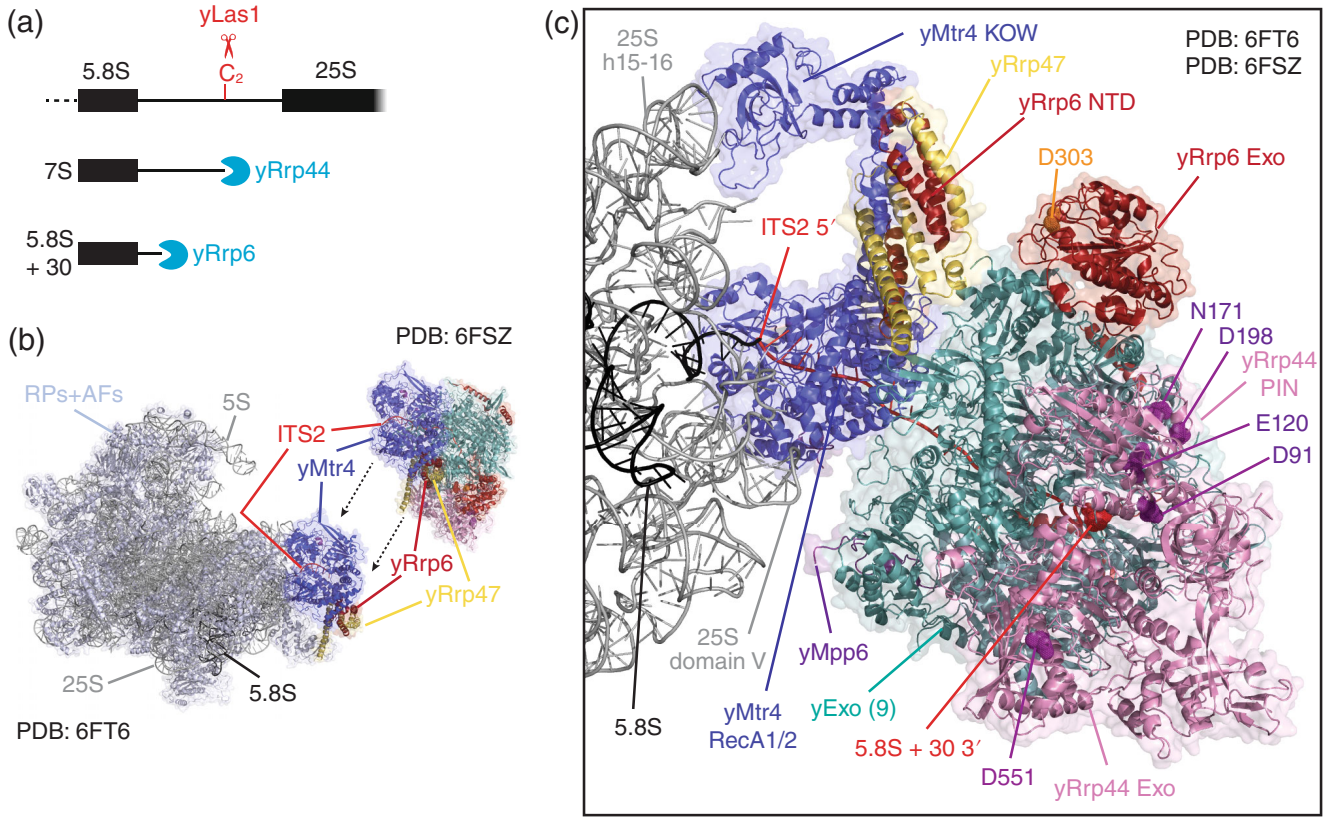

FIGURE 7 Processing towards the 3′ end of the 5.8S rRNA by the RNA exosome and co-factors. (a) Schematic view of the step-wise maturation of the 3′ end of the 5.8S rRNA in yeast following C_2 cleavage in ITS2. The 7S and 5.8S + 30 pre-rRNA intermediates are shown schematically and the enzymes responsible for their processing are indicated. (b) Cryo-EM structures of the yeast exosome 14 complex (PDB: 6FSZ), containing the core exosome (yExo9, teal), yRrp44 (pink), yRrp6 (red), yMtr4 (blue), and other co-factors, and a pre-LSU particle purified via yNop53 (PDB: 6FT6), where the exosome is stalled on a 5.8S + 30 intermediate by expression of catalytically inactive yRrp6. (c) Magnified view of the model of the complete exosome 14 complex bound to the 5.8S + 30-containing pre-60S particle. The 25S and 5S rRNAs are shown in gray, the 5.8S rRNA in black and the ITS2 fragment in red. The exosome 14 complex subunits are colored as described in panel b and shown in cartoon mode with a transparent surface view. Key contacts and catalytic domains/features are marked.

5 | CONCLUSION

Ribonucleases are key machineries mediating the processing and turnover of coding and noncoding RNAs. The new-found possibility to visualize ribonucleases together with substrate RNPs has allowed a wealth of new insights into how they identify targets and how their activities are regulated. Structural analyses of the Ski2-associated exosome and the major cytosolic 5′-3′ exoribonuclease Xrn1 in complex with mature ribosomes, purified from yeast and human cells, has illuminated mechanistic details of cytoplasmic mRNA decay (Kögel et al., 2022; Tesina et al., 2019). The parallel structure-driven insights into pre-rRNA processing events and the ribonucleases that perform them has similarly allowed a new layer of understanding of how this process is regulated. A common theme that emerges is the carefully choreographed recruitment and positioning of ribonucleases within pre-ribosomal particles. Correct assembly of appropriate binding platforms is often a pre-requisite for their recruitment, and even when bound to pre-ribosomal particles, extensive remodeling events associated with particle maturation are often necessary to bring them into contact with their pre-rRNA cleavage sites. Understanding the precise interactions of ribonucleases, both with neighboring proteins and also with their RNA substrates, is a key step toward understanding how they achieve target specificity.

While some ribonucleases required for pre-rRNA processing remain to be identified, a number of enzymes known to function in the pathway are yet to be captured on their pre-ribosomal subunits by structural analyses, despite the myriad of pre-ribosomal structures already available. For example, 5′-3′ exoribonucleolytic processing

and excised spacer fragment turnover by yRat1/hXRN2 and endoribonucleolytic cleavage of the 3′ ETS or the proximal ITS1 site A2/2a(E) have not yet been observed. In some cases, the failure to capture these structural snapshots likely reflects the transient, and potentially dynamic, nature of the interactions these enzymes make with their substrates.

This suggests that dedicated approaches to capture specific pre-rRNA processing stages or visualize particular ribonucleases in action are likely required to gain a more comprehensive overview. The strategy of enriching particles associated with ribonucleases was successfully employed for structural analyses of 5′ ETS and ITS2 processing by the yeast exosome (Lau et al., 2021; Schuller et al., 2018). Furthermore, the expression of catalytically inactive versions of ribonucleases allowed to capture the final 18S rRNA processing step by human NOB1, and the yeast exosome in action during 5.8S 3′ end maturation (Ameismeier et al., 2020; Schuller et al., 2018).

Applying such targeted approaches to other ribonucleases involved in pre-rRNA processing may enable currently "invisible" aspects of pre-rRNA processing to be illuminated. The insights gained by current structural analyses of ribonucleases in action on pre-ribosomes highlight the major advantage that the recent developments in particle-sorting during cryo-EM data analysis offer; the fact that the mixed population of complexes enriched in a single purification can be dissected into a series of maturing particles adds greatly to elucidating the series of events that regulate ribonucleases in immature particles and the steps that ultimately lead to their activation. The revolution in protein folding prediction (Jumper et al., 2021; Tunyasuvunakool et al., 2021) will likely facilitate future analyses, either by aiding density assignments during cryo-EM analyses or by driving (predicted) structure-based biochemical analyses of target recognition/specificity.

An interesting facet of pre-rRNA processing in eukaryotes is the utilization of alternative pre-rRNA processing pathways where either the same processing events take place in different order or where specific processing steps are bypassed and alternative routes are taken. Gaining insights through structural analyses into how the events involving ribonucleases are regulated holds the possibility to reveal what influences the preferential usage of one pathway over another. Also, knowledge on the mechanisms that regulate ribonucleases within pre-ribosomal particles potentially opens the door to understanding more about the dysregulation of pre-rRNA processing in disease and how ribosome assembly can be adapted in different conditions.

AUTHOR CONTRIBUTIONS

Claudia Schneider: Conceptualization (equal); visualization (supporting); writing – original draft (supporting); writing – review and editing (equal). **Katherine E. Bohnsack:** Conceptualization (equal); visualization (lead); writing – original draft (lead); writing – review and editing (equal).

ACKNOWLEDGMENT

We thank Markus Bohnsack for critical reading of the manuscript. Open Access funding enabled and organized by Projekt DEAL.

FUNDING INFORMATION

Claudia Schneider is funded by the Royal Society (Research Fellows Enhancement Award RGF\EA\180045). Katherine E. Bohnsack is supported by the Heidenreich von Siebold Programme of the University Medical Centre Göttingen.

CONFLICT OF INTEREST

All authors declare no conflicts of interest.

DATA AVAILABILITY STATEMENT

Data sharing is not applicable to this article as no new data were created or analyzed in this study.

ORCID

Claudia Schneider https://orcid.org/0000-0001-5597-2489
Katherine E. Bohnsack https://orcid.org/0000-0001-6035-4255

RELATED WIREs ARTICLES

An overview of pre-ribosomal RNA processing in eukaryotes

REFERENCES

Alderuccio, F., Chan, E. K. L., & Tan, E. M. (1991). Molecular characterization of an autoantigen of PM-Scl in the polymyositis/scleroderma overlap syndrome: A unique and complete human cDNA encoding an apparent 75-kD acidic protein of the nucleolar complex. *Journal of Experimental Medicine*, *173*(4), 941–952. https://doi.org/10.1084/jem.173.4.941

Ameismeier, M., Cheng, J., Berninghausen, O., & Beckmann, R. (2018). Visualizing late states of human 40S ribosomal subunit maturation. *Nature*, *558*(7709), 249–253. https://doi.org/10.1038/s41586-018-0193-0

Ameismeier, M., Zemp, I., van den Heuvel, J., Thoms, M., Berninghausen, O., Kutay, U., & Beckmann, R. (2020). Structural basis for the final steps of human 40S ribosome maturation. *Nature*, *587*(7835), 683–687. https://doi.org/10.1038/s41586-020-2929-x

An, W., Du, Y., & Ye, K. (2018). Structural and functional analysis of Utp24, an endonuclease for processing 18S ribosomal RNA. *PLoS One*, *13*(4), e0195723. https://doi.org/10.1371/journal.pone.0195723

Anger, A. M., Armache, J.-P., Berninghausen, O., Habeck, M., Subklewe, M., Wilson, D. N., & Beckmann, R. (2013). Structures of the human and Drosophila 80S ribosome. *Nature*, *497*(7447), 80–85. https://doi.org/10.1038/nature12104

Ansel, K. M., Pastor, W. A., Rath, N., Lapan, A. D., Glasmacher, E., Wolf, C., Smith, L. C., Papadopoulou, N., Lamperti, E. D., Tahiliani, M., Ellwart, J. W., Shi, Y., Kremmer, E., Rao, A., & Heissmeyer, V. (2008). Mouse Eri1 interacts with the ribosome and catalyzes 5.8S rRNA processing. *Nature Structural & Molecular Biology*, *15*(5), 523–530. https://doi.org/10.1038/nsmb.1417

Aubert, M., O'Donohue, M.-F., Lebaron, S., & Gleizes, P.-E. (2018). Pre-ribosomal RNA processing in human cells: From mechanisms to congenital diseases. *Biomolecules*, *8*(4), 123. https://doi.org/10.3390/biom8040123

Barandun, J., Chaker-Margot, M., Hunziker, M., Molloy, K. R., Chait, B. T., & Klinge, S. (2017). The complete structure of the small-subunit processome. *Nature Structural and Molecular Biology*, *24*(11), 944–953. https://doi.org/10.1038/nsmb.3472

Barraza-García, J., Rivera-Pedroza, C. I., Hisado-Oliva, A., Belinchón-Martínez, A., Sentchordi-Montané, L., Duncan, E. L., Clark, G. R., del Pozo, A., Ibáñez-Garikano, K., Offiah, A., Prieto-Matos, P., Cormier-Daire, V., & Heath, K. E. (2017). Broadening the phenotypic spectrum of POP1-skeletal dysplasias: Identification of POP1 mutations in a mild and severe skeletal dysplasia. *Clinical Genetics*, *92*(1), 91–98. https://doi.org/10.1111/cge.12964

Beheshtian, M., Fattahi, Z., Fadaee, M., Vazehan, R., Jamali, P., Parsimehr, E., Kamgar, M., Zonooz, M. F., Mahdavi, S. S., Kalhor, Z., Arzhangi, S., Abedini, S. S., Kermani, F. S., Mojahedi, F., Kalscheuer, V. M., Ropers, H. H., Kariminejad, A., Najmabadi, H., & Kahrizi, K. (2019). Identification of disease-causing variants in the EXOSC gene family underlying autosomal recessive intellectual disability in Iranian families. *Clinical Genetics*, *95*(March), 1–8. https://doi.org/10.1111/cge.13549

Belhabich-Baumas, K., Joret, C., Jády, B. E., Plisson-Chastang, C., Shayan, R., Klopp, C., Henras, A. K., Henry, Y., & Mougin, A. (2017). The Rio1p ATPase hinders premature entry into translation of late pre-40S pre-ribosomal particles. *Nucleic Acids Research*, *45*(18), 10824–10836. https://doi.org/10.1093/nar/gkx734

Ben-Shem, A., Garreau de Loubresse, N., Melnikov, S., Jenner, L., Yusupova, G., & Yusupov, M. (2011). SOM: The structure of the eukaryotic ribosome at 3.0 Å resolution. *Science*, *334*(6062), 1524–1529. https://doi.org/10.1126/science.1212642

Billy, E., Wegierski, T., Nasr, F., & Filipowicz, W. (2000). Rcl1p, the yeast protein similar to the RNA 3′-phosphate cyclase, associates with U3 snoRNP and is required for 18S rRNA biogenesis. *The EMBO Journal*, *19*(9), 2115–2126. https://doi.org/10.1093/emboj/19.9.2115

Bizzari, S., Hamzeh, A. R., Mohamed, M., & Al-ali, M. T. (2020). Expanded PCH1D phenotype linked to EXOSC9 mutation. *European Journal of Medical Genetics*, *63*(1), 103622. https://doi.org/10.1016/j.ejmg.2019.01.012

Bleichert, F., Granneman, S., Osheim, Y. N., Beyer, A. L., & Baserga, S. J. (2006). The PINc domain protein Utp24, a putative nuclease, is required for the early cleavage steps in 18S rRNA maturation. *Proceedings of the National Academy of Sciences of the United States of America*, *103*(25), 9464–9469. https://doi.org/10.1073/pnas.0603673103

Blüthner, M., & Bautz, F. A. (1992). Cloning and characterization of the cDNA coding for a polymyositis-scleroderma overlap syndrome-related nucleolar 100-kD protein. *The Journal of Experimental Medicine*, *176*(4), 973–980. https://doi.org/10.1084/jem.176.4.973

Boczonadi, V., Mu, J. S., Pyle, A., Munkley, J., Dor, T., Quartararo, J., Ferrero, I., Karcagi, V., Giunta, M., Polvikoski, T., Birchall, D., Princzinger, A., Cinnamon, Y., Lützkendorf, S., Piko, H., Reza, M., Florez, L., Santibanez-Koref, M., Griffin, H., … Horvath, R. (2014). EXOSC8 mutations alter mRNA metabolism and cause hypomyelination with spinal muscular atrophy and cerebellar hypoplasia. *Nature Communications*, *5*, 4287. https://doi.org/10.1038/ncomms5287

Bohnsack, K. E., & Bohnsack, M. T. (2019). Uncovering the assembly pathway of human ribosomes and its emerging links to disease. *The EMBO Journal*, *38*, e100278. https://doi.org/10.15252/embj.2018100278

Bonafé, L., Schmitt, K., Eich, G., Giedion, A., & Superti-Furga, A. (2002). RMRP gene sequence analysis confirms a cartilage-hair hypoplasia variant with only skeletal manifestations and reveals a high density of single-nucleotide polymorphisms. *Clinical Genetics*, *61*(2), 146–151. https://doi.org/10.1034/j.1399-0004.2002.610210.x

Bonneau, F., Basquin, J., Ebert, J., Lorentzen, E., & Conti, E. (2009). The yeast exosome functions as a macromolecular cage to channel RNA substrates for degradation. *Cell*, *139*(3), 547–559. https://doi.org/10.1016/j.cell.2009.08.042

Briggs, M. W., Burkard, K. T., & Butler, J. S. (1998). Rrp6p, the yeast homologue of the human PM-Scl 100-kDa autoantigen, is essential for efficient 5.8 S rRNA 3′ end formation. *The Journal of Biological Chemistry*, *273*(21), 13255–13263. https://doi.org/10.1074/jbc.273.21.13255

Burns, D. T., Donkervoort, S., Müller, J. S., Knierim, E., Bharucha-Goebel, D., Faqeih, E. A., Bell, S. K., AlFaifi, A. Y., Monies, D., Millan, F., Retterer, K., Dyack, S., MacKay, S., Morales-Gonzalez, S., Giunta, M., Munro, B., Hudson, G., Scavina, M., Baker, L., … Bönnemann, C. G. (2018). Variants in EXOSC9 disrupt the RNA exosome and result in cerebellar atrophy with spinal motor neuronopathy. *American Journal of Human Genetics*, *102*(5), 858–873. https://doi.org/10.1016/j.ajhg.2018.03.011

Butterfield, R. J., Stevenson, T. J., Xing, L., Newcomb, T. M., Nelson, B., Zeng, W., Li, X., Lu, H. M., Lu, H., Farwell Gonzalez, K. D., Wei, J. P., Chao, E. C., Prior, T. W., Snyder, P. J., Bonkowsky, J. L., & Swoboda, K. J. (2014). Congenital lethal motor neuron disease with a novel defect in ribosome biogenesis. *Neurology*, *82*(15), 1322–1330. https://doi.org/10.1212/WNL.0000000000000305

Calame, D. G., Herman, I., Fatih, J. M., Du, H., Akay, G., Jhangiani, S. N., Coban-Akdemir, Z., Milewicz, D. M., Gibbs, R. A., Posey, J. E., Marafi, D., Hunter, J. V., Fan, Y., Lupski, J. R., & Miyake, C. Y. (2021). Risk of sudden cardiac death in EXOSC5-related disease. *American Journal of Medical Genetics, Part A*, *185*, 1–9. https://doi.org/10.1002/ajmg.a.62352

Castle, C. D., Cassimere, E. K., & Denicourt, C. (2012). LAS1L interacts with the mammalian Rix1 complex to regulate ribosome biogenesis. *Molecular Biology of the Cell*, *23*(4), 716–728. https://doi.org/10.1091/mbc.E11-06-0530

Castle, C. D., Cassimere, E. K., Lee, J., & Denicourt, C. (2010). Las1L is a nucleolar protein required for cell proliferation and ribosome biogenesis. *Molecular and Cellular Biology*, *30*(18), 4404–4414. https://doi.org/10.1128/MCB.00358-10

Castle, C. D., Sardana, R., Dandekar, V., Borgianini, V., Johnson, A. W., & Denicourt, C. (2013). Las1 interacts with Grc3 polynucleotide kinase and is required for ribosome synthesis in Saccharomyces cerevisiae. *Nucleic Acids Research*, *41*(2), 1135–1150. https://doi.org/10.1093/nar/gks1086

Cerezo, E., Plisson-Chastang, C., Henras, A. K., Lebaron, S., Gleizes, P.-E., O'Donohue, M.-F., Romeo, Y., & Henry, Y. (2019). Maturation of pre-40S particles in yeast and humans. *Wiley Interdisciplinary Reviews: RNA*, *10*(1), e1516. https://doi.org/10.1002/wrna.1516

Chaker-Margot, M., Barandun, J., Hunziker, M., & Klinge, S. (2017). Architecture of the yeast small subunit processome. *Science*, *355*(6321), eaal1880. https://doi.org/10.1126/science.aal1880

Chaker-Margot, M., Hunziker, M., Barandun, J., Dill, B. D., & Klinge, S. (2015). Stage-specific assembly events of the 6-MDa small-subunit processome initiate eukaryotic ribosome biogenesis. *Nature Structural & Molecular Biology*, *22*(11), 920–923. https://doi.org/10.1038/nsmb.3111

Chang, J. H., Xiang, S., Xiang, K., Manley, J. L., & Tong, L. (2011). Structural and biochemical studies of the 5′→3′ exoribonuclease Xrn1. *Nature Structural and Molecular Biology*, *18*(3), 270–276. https://doi.org/10.1038/nsmb.1984

Chapman, M. A., Lawrence, M. S., Keats, J. J., Cibulskis, K., Sougnez, C., Schinzel, A. C., Harview, C. L., Brunet, J. P., Ahmann, G. J., Adli, M., Anderson, K. C., Ardlie, K. G., Auclair, D., Baker, A., Bergsagel, P. L., Bernstein, B. E., Drier, Y., Fonseca, R., Gabriel, S. B., ... Golub, T. R. (2011). Initial genome sequencing and analysis of multiple myeloma. *Nature*, *471*(7339), 467–472. https://doi.org/10.1038/nature09837

Chen, Y., Hao, Q., Wang, S., Cao, M., Huang, Y., Weng, X., Wang, J., Zhang, Z., He, X., Lu, H., & Zhou, X. (2021). Inactivation of the tumor suppressor p53 by long noncoding RNA RMRP. *Proceedings of the National Academy of Sciences of the United States of America*, *118*(29), e2026813118. https://doi.org/10.1073/pnas.2026813118

Cheng, J., Lau, B., La Venuta, G., Ameismeier, M., Berninghausen, O., Hurt, E., & Beckmann, R. (2020). 90S pre-ribosome transformation into the primordial 40S subunit. *Science*, *369*(6510), 1470–1476. https://doi.org/10.1126/science.abb4119

Choque, E., Schneider, C., Gadal, O., & Dez, C. (2018). Turnover of aberrant pre-40S pre-ribosomal particles is initiated by a novel endonucleolytic decay pathway. *Nucleic Acids Research*, *46*(9), 4699–4714. https://doi.org/10.1093/nar/gky116

Chu, S., Archer, R. H., Zengel, J. M., & Lindahl, L. (1994). The RNA of RNase MRP is required for normal processing of ribosomal RNA. *Proceedings of the National Academy of Sciences of the United States of America*, *91*(2), 659–663. https://doi.org/10.1073/pnas.91.2.659

Ciganda, M., & Williams, N. (2011). Eukaryotic 5S rRNA biogenesis. *Wiley Interdisciplinary Reviews: RNA*, *2*(4), 523–533. https://doi.org/10.1002/wrna.74

Coute, Y., Kindbeiter, K., Belin, S., Dieckmann, R., Duret, L., Bezin, L., Sanchez, J.-C., & Diaz, J.-J. (2008). ISG20L2, a novel vertebrate nucleolar exoribonuclease involved in ribosome biogenesis. *Molecular & Cellular Proteomics: MCP*, *7*(3), 546–559. https://doi.org/10.1074/mcp.M700510-MCP200

Daniels, P. W., Hama Soor, T., Levicky, Q., Hettema, E. H., & Mitchell, P. (2022). Contribution of domain structure to the function of the yeast DEDD family exoribonuclease and RNase T functional homolog, Rex1. *RNA*, *28*(4), 493–507. https://doi.org/10.1261/rna.078939.121

Das, M., Zattas, D., Zinder, J. C., Wasmuth, E. V., Henri, J., & Lima, C. D. (2021). Substrate discrimination and quality control require each catalytic activity of TRAMP and the nuclear RNA exosome. *Proceedings of the National Academy of Sciences of the United States of America*, *118*(14), e2024846118. https://doi.org/10.1073/pnas.2024846118

Davidson, L., Francis, L., Cordiner, R. A., Eaton, J. D., Estell, C., Macias, S., Cáceres, J. F., & West, S. (2019). Rapid depletion of DIS3, EXOSC10, or XRN2 reveals the immediate impact of exoribonucleolysis on nuclear RNA metabolism and transcriptional control. *Cell Reports*, *26*(10), 2779–2791. https://doi.org/10.1016/j.celrep.2019.02.012

Delan-Forino, C., Schneider, C., & Tollervey, D. (2017). Transcriptome-wide analysis of alternative routes for RNA substrates into the exosome complex. *PLoS Genetics*, *13*(3), e1006699. https://doi.org/10.1371/journal.pgen.1006699

Dhanraj, S., Gunja, S. M. R., Deveau, A. P., Nissbeck, M., Boonyawat, B., Coombs, A. J., Renieri, A., Mucciolo, M., Marozza, A., Buoni, S., Turner, L., Li, H., Jarrar, A., Sabanayagam, M., Kirby, M., Shago, M., Pinto, D., Berman, J. N., Scherer, S. W., ... Dror, Y. (2015). Bone marrow failure and developmental delay caused by mutations in poly(A)-specific ribonuclease (PARN). *Journal of Medical Genetics*, *52*(11), 738–748. https://doi.org/10.1136/jmedgenet-2015-103292

Di Donato, N., Neuhann, T., Kahlert, A., Klink, B., Hackmann, K., Neuhann, I., Novotna, B., Schallner, J., Krause, C., Glass, I. A., Parnell, S. E., Benet-Pages, A., Nissen, A. M., Berger, W., Altmüller, J., Thiele, H., Weber, B. H. F., Schrock, E., Dobyns, W. B., ... Rump, A. (2016). Mutations in EXOSC2 are associated with a novel syndrome characterised by retinitis pigmentosa, progressive hearing

loss, premature ageing, short stature, mild intellectual disability and distinctive gestalt. *Journal of Medical Genetics*, *53*, 419–425. https://doi.org/10.1136/jmedgenet-2015-103511

Ding, L., Ley, T. J., Larson, D. E., Miller, C. A., Koboldt, D. C., Welch, J. S., Ritchey, J. K., Young, M. A., Lamprecht, T., McLellan, M. D., McMichael, J. F., Wallis, J. W., Lu, C., Shen, D., Harris, C. C., Dooling, D. J., Fulton, R. S., Fulton, L. L., Chen, K., … DiPersio, J. F. (2012). Clonal evolution in relapsed acute myeloid leukaemia revealed by whole-genome sequencing. *Nature*, *481*(7382), 506–510. https://doi.org/10.1038/nature10738

Drazkowska, K., Tomecki, R., Stodus, K., Kowalska, K., Czarnocki-Cieciura, M., & Dziembowski, A. (2013). The RNA exosome complex central channel controls both exonuclease and endonuclease Dis3 activities in vivo and in vitro. *Nucleic Acids Research*, *41*(6), 3845–3858. https://doi.org/10.1093/nar/gkt060

Du, Y., An, W., Zhu, X., Sun, Q., Qi, J., & Ye, K. (2020). Cryo-EM structure of 90S small ribosomal subunit precursors in transition states. *Science*, *369*(6510), 1477–1481. https://doi.org/10.1126/science.aba9690

Dziembowski, A., Lorentzen, E., Conti, E., & Séraphin, B. (2007). A single subunit, Dis3, is essentially responsible for yeast exosome core activity. *Nature Structural & Molecular Biology*, *14*(1), 15–22. https://doi.org/10.1038/nsmb1184

Eder, P. S., Kekuda, R., Stolc, V., & Altman, S. (1997). Characterization of two scleroderma autoimmune antigens that copurify with human ribonuclease P. *Proceedings of the National Academy of Sciences of the United States of America*, *94*(4), 1101–1106. https://doi.org/10.1073/pnas.94.4.1101

Elalaoui, S. C., Laarabi, F. Z., Mansouri, M., Mrani, N. A., Nishimura, G., & Sefiani, A. (2016). Further evidence of POP1 mutations as the cause of anauxetic dysplasia. *American Journal of Medical Genetics, Part A*, *170*(9), 2462–2465. https://doi.org/10.1002/ajmg.a.37839

Elela, S. A., Igel, H., & Ares, M. J. (1996). RNase III cleaves eukaryotic preribosomal RNA at a U3 snoRNP-dependent site. *Cell*, *85*(1), 115–124. https://doi.org/10.1016/s0092-8674(00)81087-9

Eppens, N. A., Faber, A. W., Rondaij, M., Jahangir, R. S., van Hemert, S., Vos, J. C., Venema, J., & Raué, H. A. (2002). Deletions in the S1 domain of Rrp5p cause processing at a novel site in ITS1 of yeast pre-rRNA that depends on Rex4p. *Nucleic Acids Research*, *30*(19), 4222–4231. https://doi.org/10.1093/nar/gkf538

Esakova, O., & Krasilnikov, A. S. (2010). Of proteins and RNA: The RNase P/MRP family. *RNA*, *16*(9), 1725–1747. https://doi.org/10.1261/rna.2214510

Esakova, O., Perederina, A., Berezin, I., & Krasilnikov, A. S. (2013). Conserved regions of ribonucleoprotein ribonuclease MRP are involved in interactions with its substrate. *Nucleic Acids Research*, *41*(14), 7084–7091. https://doi.org/10.1093/nar/gkt432

Faber, A. W., Van Dijk, M., Raué, H. A., & Vos, J. C. (2002). Ngl2p is a Ccr4p-like RNA nuclease essential for the final step in 3′-end processing of 5.8S rRNA in Saccharomyces cerevisiae. *RNA*, *8*(9), 1095–1101. https://doi.org/10.1017/s1355838202021027

Faber, A. W., Vos, J. C., Vos, H. R., Ghazal, G., Elela, S. A., & Raué, H. A. (2004). The RNA catabolic enzymes Rex4p, Rnt1p, and Dbr1p show genetic interaction with trans-acting factors involved in processing of ITS1 in Saccharomyces cerevisiae pre-rRNA. *RNA*, *10*(12), 1946–1956. https://doi.org/10.1261/rna.7155904

Falk, S., Bonneau, F., Ebert, J., Kögel, A., & Conti, E. (2017). Mpp6 incorporation in the nuclear exosome contributes to RNA channeling through the Mtr4 helicase. *Cell Reports*, *20*(10), 2279–2286. https://doi.org/10.1016/j.celrep.2017.08.033

Fatica, A., Oeffinger, M., Dlakić, M., & Tollervey, D. (2003). Nob1p is required for cleavage of the 3′ end of 18S rRNA. *Molecular and Cellular Biology*, *23*(5), 1798–1807. https://doi.org/10.1128/MCB.23.5.1798-1807.2003

Fatica, A., Tollervey, D., & Dlakić, M. (2004). PIN domain of Nob1p is required for D-site cleavage in 20S pre-rRNA. *RNA*, *10*(11), 1698–1701. https://doi.org/10.1261/rna.7123504

Fromm, L., Falk, S., Flemming, D., Schuller, J. M., Thoms, M., Conti, E., & Hurt, E. (2017). Reconstitution of the complete pathway of ITS2 processing at the pre-ribosome. *Nature Communications*, *8*(1), 1787. https://doi.org/10.1038/s41467-017-01786-9

Gabel, H. W., & Ruvkun, G. (2008). The exonuclease ERI-1 has a conserved dual role in 5.8S rRNA processing and RNAi. *Nature Structural & Molecular Biology*, *15*(5), 531–533. https://doi.org/10.1038/nsmb.1411

Gasse, L., Flemming, D., & Hurt, E. (2015). Coordinated ribosomal ITS2 RNA processing by the Las1 complex integrating endonuclease, polynucleotide kinase, and exonuclease activities. *Molecular Cell*, *60*(5), 808–815. https://doi.org/10.1016/j.molcel.2015.10.021

Gerlach, P., Schuller, J. M., Bonneau, F., Basquin, J., Reichelt, P., Falk, S., & Conti, E. (2018). Distinct and evolutionary conserved structural features of the human nuclear exosome complex. *eLife*, *7*, 7. https://doi.org/10.7554/eLife.38686

Gill, T., Cai, T., Aulds, J., Wierzbicki, S., & Schmitt, M. E. (2004). RNase MRP cleaves the CLB2 mRNA to promote cell cycle progression: Novel method of mRNA degradation. *Molecular and Cellular Biology*, *24*(3), 945–953. https://doi.org/10.1128/MCB.24.3.945-953.2004

Glazov, E. A., Zankl, A., Donskoi, M., Kenna, T. J., Thomas, G. P., Clark, G. R., Duncan, E. L., & Brown, M. A. (2011). Whole-exome re-sequencing in a family quartet identifies POP1 mutations as the cause of a novel skeletal dysplasia. *PLoS Genetics*, *7*(3), 1–7. https://doi.org/10.1371/journal.pgen.1002027

Goldfarb, K. C., & Cech, T. R. (2017). Targeted CRISPR disruption reveals a role for RNase MRP RNA in human preribosomal RNA processing. *Genes & Development*, *31*(1), 59–71. https://doi.org/10.1101/gad.286963.116

Granneman, S., Petfalski, E., & Tollervey, D. (2011). A cluster of ribosome synthesis factors regulate pre-rRNA folding and 5.8S rRNA maturation by the Rat1 exonuclease. *The EMBO Journal*, *30*(19), 4006–4019. https://doi.org/10.1038/emboj.2011.256

Gudipati, R. K., Xu, Z., Lebreton, A., Séraphin, B., Steinmetz, L. M., Jacquier, A., & Libri, D. (2012). Extensive degradation of RNA precursors by the exosome in wild-type cells. *Molecular Cell*, *48*(3), 409–421. https://doi.org/10.1016/j.molcel.2012.08.018

Han, J., & van Hoof, A. (2016). The RNA exosome channeling and direct access conformations have distinct In vivo functions. *Cell Reports*, *16*(12), 3348–3358. https://doi.org/10.1016/j.celrep.2016.08.059

Hector, R. D., Burlacu, E., Aitken, S., Le Bihan, T., Tuijtel, M., Zaplatina, A., Cook, A. G., & Granneman, S. (2014). Snapshots of pre-rRNA structural flexibility reveal eukaryotic 40S assembly dynamics at nucleotide resolution. *Nucleic Acids Research*, *42*(19), 12138–12154. https://doi.org/10.1093/nar/gku815

Henras, A. K., Plisson-Chastang, C., O'Donohue, M.-F., Chakraborty, A., & Gleizes, P.-E. (2015). An overview of pre-ribosomal RNA processing in eukaryotes. *Wiley Interdisciplinary Reviews: RNA*, *6*(2), 225–242. https://doi.org/10.1002/wrna.1269

Henry, Y., Wood, H., Morrissey, J. P., Petfalski, E., Kearsey, S., & Tollervey, D. (1994). The 5′ end of yeast 5.8S rRNA is generated by exonucleases from an upstream cleavage site. *The EMBO Journal*, *13*(10), 2452–2463. https://doi.org/10.1002/j.1460-2075.1994.tb06530.x

Heuer, A., Thomson, E., Schmidt, C., Berninghausen, O., Becker, T., Hurt, E., & Beckmann, R. (2017). Cryo-EM structure of a late pre-40S ribosomal subunit from Saccharomyces cerevisiae. *eLife*, *6*, e30189. https://doi.org/10.7554/eLife.30189

Hoareau-Aveilla, C., Fayet-Lebaron, E., Jády, B. E., Henras, A. K., & Kiss, T. (2012). Utp23p is required for dissociation of snR30 small nucleolar RNP from preribosomal particles. *Nucleic Acids Research*, *40*(8), 3641–3652. https://doi.org/10.1093/nar/gkr1213

Hojka-Osinska, A., Chlebowski, A., Grochowska, J., Owczarek, E. P., Affek, K., Kłosowska-Kosicka, K., Szczesny, R. J., & Dziembowski, A. (2021). Landscape of functional interactions of human processive ribonucleases revealed by high-throughput siRNA screenings. *IScience*, *24*(9), 103036. https://doi.org/10.1016/j.isci.2021.103036

Horn, D. M., Mason, S. L., & Karbstein, K. (2011). Rcl1 protein, a novel nuclease for 18 S ribosomal RNA production. *The Journal of Biological Chemistry*, *286*(39), 34082–34087. https://doi.org/10.1074/jbc.M111.268649

Hunziker, M., Barandun, J., Buzovetsky, O., Steckler, C., Molina, H., & Klinge, S. (2019). Conformational switches control early maturation of the eukaryotic small ribosomal subunit. *eLife*, *8*, e45185. https://doi.org/10.7554/eLife.45185

Hurtig, J. E., & van Hoof, A. (2022). Yeast Dxo1 is required for 25S rRNA maturation and acts as a transcriptome-wide distributive exonuclease. *RNA*, *28*(5), 657–667. https://doi.org/10.1261/rna.078952.121

Jackson, R. N., Klauer, A. A., Hintze, B. J., Robinson, H., van Hoof, A., & Johnson, S. J. (2010). The crystal structure of Mtr4 reveals a novel arch domain required for rRNA processing. *The EMBO Journal*, *29*(13), 2205–2216. https://doi.org/10.1038/emboj.2010.107

Januszyk, K., Liu, Q., & Lima, C. D. (2011). Activities of human RRP6 and structure of the human RRP6 catalytic domain. *RNA*, *17*(8), 1566–1577. https://doi.org/10.1261/rna.2763111

Jinek, M., Coyle, S. M., & Doudna, J. A. (2011). Coupled 5′ nucleotide recognition and processivity in Xrn1-mediated mRNA decay. *Molecular Cell*, *41*(5), 600–608. https://doi.org/10.1016/j.molcel.2011.02.004

Jumper, J., Evans, R., Pritzel, A., Green, T., Figurnov, M., Ronneberger, O., Tunyasuvunakool, K., Bates, R., Žídek, A., Potapenko, A., Bridgland, A., Meyer, C., Kohl, S. A. A., Ballard, A. J., Cowie, A., Romera-Paredes, B., Nikolov, S., Jain, R., Adler, J., … Hassabis, D. (2021). Highly accurate protein structure prediction with AlphaFold. *Nature*, *596*(7873), 583–589. https://doi.org/10.1038/s41586-021-03819-2

Kater, L., Mitterer, V., Thoms, M., Cheng, J., Berninghausen, O., Beckmann, R., & Hurt, E. (2020). Construction of the central protuberance and L1 stalk during 60S subunit biogenesis. *Molecular Cell*, *79*(4), 615–628.e5. https://doi.org/10.1016/j.molcel.2020.06.032

Kobyłecki, K., Drążkowska, K., Kuliński, T. M., Dziembowski, A., & Tomecki, R. (2018). Elimination of 01/A′-A0 pre-rRNA processing by-product in human cells involves cooperative action of two nuclear exosome-associated nucleases: RRP6 and DIS3. *RNA*, *24*(12), 1677–1692. https://doi.org/10.1261/rna.066589.118

Kögel, A., Keidel, A., Bonneau, F., Schäfer, I. B., & Conti, E. (2022). The human SKI complex regulates channeling of ribosome-bound RNA to the exosome via an intrinsic gatekeeping mechanism. *Molecular Cell*, *82*(4), 756–769.e8. https://doi.org/10.1016/j.molcel.2022.01.009

Kornprobst, M., Turk, M., Kellner, N., Cheng, J., Flemming, D., Koš-Braun, I., Koš, M., Thoms, M., Berninghausen, O., Beckmann, R., & Hurt, E. (2016). Architecture of the 90S pre-ribosome: A structural view on the birth of the eukaryotic ribosome. *Cell*, *166*(2), 380–393. https://doi.org/10.1016/j.cell.2016.06.014

Kufel, J., Dichtl, B., & Tollervey, D. (1999). Yeast Rnt1p is required for cleavage of the pre-ribosomal RNA in the 3′ ETS but not the 5′ ETS. *RNA*, *5*(7), 909–917.

Lamanna, A. C., & Karbstein, K. (2009). Nob1 binds the single-stranded cleavage site D at the 3′-end of 18S rRNA with its PIN domain. *Proceedings of the National Academy of Sciences of the United States of America*, *106*(34), 14259–14264. https://doi.org/10.1073/pnas.0905403106

Lan, P., Zhou, B., Tan, M., Li, S., Cao, M., Wu, J., & Lei, M. (2020). Structural insight into precursor ribosomal RNA processing by ribonuclease MRP. *Science*, *369*(6504), 656–663. https://doi.org/10.1126/science.abc0149

Lau, B., Cheng, J., Flemming, D., La Venuta, G., Berninghausen, O., Beckmann, R., & Hurt, E. (2021). Structure of the maturing 90S pre-ribosome in association with the RNA exosome. *Molecular Cell*, *81*(2), 293–303.e4. https://doi.org/10.1016/j.molcel.2020.11.009

Lebaron, S., Schneider, C., van Nues, R. W., Swiatkowska, A., Walsh, D., Böttcher, B., Granneman, S., Watkins, N. J., & Tollervey, D. (2012). Proofreading of pre-40S ribosome maturation by a translation initiation factor and 60S subunits. *Nature Structural & Molecular Biology*, *19*(8), 744–753. https://doi.org/10.1038/nsmb.2308

Lebreton, A., Tomecki, R., Dziembowski, A., & Séraphin, B. (2008). Endonucleolytic RNA cleavage by a eukaryotic exosome. *Nature*, *456*(7224), 993–996. https://doi.org/10.1038/nature07480

Li, X., Zengel, J. M., & Lindahl, L. (2021). A novel model for the RNase MRP-induced switch between the formation of different forms of 5.8S rRNA. *International Journal of Molecular Sciences*, *22*(13), 6690. https://doi.org/10.3390/ijms22136690

Li, X., Zaman, S., Langdon, Y., Zengel, J. M., & Lindahl, L. (2004). Identification of a functional core in the RNA component of RNase MRP of budding yeasts. *Nucleic Acids Research*, *32*(12), 3703–3711. https://doi.org/10.1093/nar/gkh689

Liang, Y. H., Lavoie, M., Comeau, M. A., Elela, S. A., & Ji, X. (2014). Structure of a eukaryotic RNase III Postcleavage complex reveals a double-ruler mechanism for substrate selection. *Molecular Cell*, *54*(3), 431–444. https://doi.org/10.1016/j.molcel.2014.03.006

Lindahl, L., Bommankanti, A., Li, X., Hayden, L., Jones, A., Khan, M., Oni, T., & Zengel, J. M. (2009). RNase MRP is required for entry of 35S precursor rRNA into the canonical processing pathway. *RNA*, *15*(7), 1407–1416. https://doi.org/10.1261/rna.1302909

Lingaraju, M., Johnsen, D., Schlundt, A., Langer, L. M., Basquin, J., Sattler, M., Heick Jensen, T., Falk, S., & Conti, E. (2019). The MTR4 helicase recruits nuclear adaptors of the human RNA exosome using distinct arch-interacting motifs. *Nature Communications*, *10*(1), 3393. https://doi.org/10.1038/s41467-019-11339-x

Lingaraju, M., Schuller, J. M., Falk, S., Gerlach, P., Bonneau, F., Basquin, J., Benda, C., & Conti, E. (2019). To process or to decay: A mechanistic view of the nuclear RNA exosome. *Cold Spring Harbor Symposia on Quantitative Biology*, *84*, 155–163. https://doi.org/10.1101/sqb.2019.84.040295

Liu, J.-J., Bratkowski, M. A., Liu, X., Niu, C.-Y., Ke, A., & Wang, H.-W. (2014). Visualization of distinct substrate-recruitment pathways in the yeast exosome by EM. *Nature Structural & Molecular Biology*, *21*(1), 95–102. https://doi.org/10.1038/nsmb.2736

Liu, Q., Greimann, J. C., & Lima, C. D. (2006). Reconstitution, activities, and structure of the eukaryotic RNA exosome. *Cell*, *127*(6), 1223–1237. https://doi.org/10.1016/j.cell.2006.10.037

Lorentzen, E., Basquin, J., Tomecki, R., Dziembowski, A., & Conti, E. (2008). Structure of the active subunit of the yeast exosome core, Rrp44: Diverse modes of substrate recruitment in the RNase II nuclease family. *Molecular Cell*, *29*(6), 717–728. https://doi.org/10.1016/j.molcel.2008.02.018

Lu, J., Sun, M., & Ye, K. (2013). Structural and functional analysis of Utp23, a yeast ribosome synthesis factor with degenerate PIN domain. *RNA*, *19*(12), 1815–1824. https://doi.org/10.1261/rna.040808.113

Lygerou, Z., Mitchell, P., Petfalski, E., Séraphin, B., & Tollervey, D. (1994). The POP1 gene encodes a protein component common to the RNase MRP and RNase P ribonucleoproteins. *Genes & Development*, *8*(12), 1423–1433. https://doi.org/10.1101/gad.8.12.1423

Lygerou, Z., Pluk, H., Van Venrooij, W. J., & Séraphin, B. (1996). hPop1: An autoantigenic protein subunit shared by the human RNase P and RNase MRP ribonucleoproteins. *EMBO Journal*, *15*(21), 5936–5948. https://doi.org/10.1002/j.1460-2075.1996.tb00980.x

Madru, C., Lebaron, S., Blaud, M., Delbos, L., Pipoli, J., Pasmant, E., Réty, S., & Leulliot, N. (2015). Chaperoning 5S RNA assembly. *Genes & Development*, *29*(13), 1432–1446. https://doi.org/10.1101/gad.260349.115

Makino, D. L., Baumgärtner, M., & Conti, E. (2013). Crystal structure of an RNA-bound 11-subunit eukaryotic exosome complex. *Nature*, *495*(7439), 70–75. https://doi.org/10.1038/nature11870

Makino, D. L., Schuch, B., Stegmann, E., Baumgärtner, M., Basquin, C., & Conti, E. (2015). RNA degradation paths in a 12-subunit nuclear exosome complex. *Nature*, *524*(7563), 54–58. https://doi.org/10.1038/nature14865

Malet, H., Topf, M., Clare, D. K., Ebert, J., Bonneau, F., Basquin, J., Drazkowska, K., Tomecki, R., Dziembowski, A., Conti, E., Saibil, H. R., & Lorentzen, E. (2010). RNA channelling by the eukaryotic exosome. *EMBO Reports*, *11*(12), 936–942. https://doi.org/10.1038/embor.2010.164

Mattijssen, S., Hinson, E. R., Onnekink, C., Hermanns, P., Zabel, B., Cresswell, P., & Pruijn, G. J. M. (2011). Viperin mRNA is a novel target for the human RNase MRP/RNase P endoribonuclease. *Cellular and Molecular Life Sciences: CMLS*, *68*(14), 2469–2480. https://doi.org/10.1007/s00018-010-0568-3

Milligan, L., Decourty, L., Saveanu, C., Rappsilber, J., Ceulemans, H., Jacquier, A., & Tollervey, D. (2008). A yeast exosome cofactor, Mpp6, functions in RNA surveillance and in the degradation of noncoding RNA transcripts. *Molecular and Cellular Biology*, *28*(17), 5446–5457. https://doi.org/10.1128/MCB.00463-08

Mitchell, P., Petfalski, E., Shevchenko, A., Mann, M., & Tollervey, D. (1997). The exosome: A conserved eukaryotic RNA processing complex containing multiple 3′-->5′ exoribonucleases. *Cell*, *91*(4), 457–466. https://doi.org/10.1016/s0092-8674(00)80432-8

Mitchell, P., Petfalski, E., Houalla, R., Podtelejnikov, A., Mann, M., & Tollervey, D. (2003). Rrp47p is an exosome-associated protein required for the 3′ processing of stable RNAs. *Molecular and Cellular Biology*, *23*(19), 6982–6992. https://doi.org/10.1128/MCB.23.19.6982-6992.2003

Mitterer, V., Shayan, R., Ferreira-Cerca, S., Murat, G., Enne, T., Rinaldi, D., Weigl, S., Omanic, H., Gleizes, P. E., Kressler, D., Plisson-Chastang, C., & Pertschy, B. (2019). Conformational proofreading of distant 40S ribosomal subunit maturation events by a long-range communication mechanism. *Nature Communications*, *10*(1), 2754. https://doi.org/10.1038/s41467-019-10678-z

Montellese, C., Montel-Lehry, N., Henras, A. K., Kutay, U., Gleizes, P.-E., & O'Donohue, M.-F. (2017). Poly(A)-specific ribonuclease is a nuclear ribosome biogenesis factor involved in human 18S rRNA maturation. *Nucleic Acids Research*, *45*, 6822–6836. https://doi.org/10.1093/nar/gkx253

Mullineux, S.-T., & Lafontaine, D. L. J. (2012). Mapping the cleavage sites on mammalian pre-rRNAs: Where do we stand? *Biochimie*, *94*(7), 1521–1532. https://doi.org/10.1016/j.biochi.2012.02.001

Oeffinger, M., Zenklusen, D., Ferguson, A., Wei, K. E., El Hage, A., Tollervey, D., Chait, B. T., Singer, R. H., & Rout, M. P. (2009). Rrp17p is a eukaryotic exonuclease required for 5′ end processing of pre-60S ribosomal RNA. *Molecular Cell*, *36*(5), 768–781. https://doi.org/10.1016/j.molcel.2009.11.011

Overbeck, J. H., Stelzig, D., Fuchs, A.-L., Wurm, J. P., & Sprangers, R. (2022). Observation of conformation changes that underlie the catalytic cycle of Xrn2. *Nature Chemical Biology*, *18*, 1152–1160. https://doi.org/10.1038/s41589-022-01111-6

Perederina, A., Li, D., Lee, H., Bator, C., Berezin, I., Hafenstein, S. L., & Krasilnikov, A. S. (2020). Cryo-EM structure of catalytic ribonucleoprotein complex RNase MRP. *Nature Communications*, *11*(1), 3474. https://doi.org/10.1038/s41467-020-17308-z

Pertschy, B., Schneider, C., Gnadig, M., Schafer, T., Tollervey, D., & Hurt, E. (2009). RNA helicase Prp43 and its co-factor Pfa1 promote 20 to 18 S rRNA processing catalyzed by the endonuclease Nob1. *The Journal of Biological Chemistry*, *284*(50), 35079–35091. https://doi.org/10.1074/jbc.M109.040774

Petfalski, E., Dandekar, T., Henry, Y., & Tollervey, D. (1998). Processing of the precursors to small nucleolar RNAs and rRNAs requires common components. *Molecular and Cellular Biology*, *18*(3), 1181–1189. https://doi.org/10.1128/mcb.18.3.1181

Pillon, M. C., Hsu, A. L., Krahn, J. M., Williams, J. G., Goslen, K. H., Sobhany, M., Borgnia, M. J., & Stanley, R. E. (2019). Cryo-EM reveals active site coordination within a multienzyme pre-rRNA processing complex. *Nature Structural & Molecular Biology*, *26*(9), 830–839. https://doi.org/10.1038/s41594-019-0289-8

Pillon, M. C., Sobhany, M., Borgnia, M. J., Williams, J. G., & Stanley, R. E. (2017). Grc3 programs the essential endoribonuclease Las1 for specific RNA cleavage. *Proceedings of the National Academy of Sciences of the United States of America*, *114*(28), E5530–E5538. https://doi.org/10.1073/pnas.1703133114

Pirouz, M., Munafò, M., Ebrahimi, A. G., Choe, J., & Gregory, R. I. (2019). Exonuclease requirements for mammalian ribosomal RNA biogenesis and surveillance. *Nature Structural & Molecular Biology*, *26*(6), 490–500. https://doi.org/10.1038/s41594-019-0234-x

Plassart, L., Shayan, R., Montellese, C., Rinaldi, D., Larburu, N., Pichereaux, C., Froment, C., Lebaron, S., O'Donohue, M. F., Kutay, U., Marcoux, J., Gleizes, P. E., & Plisson-Chastang, C. (2021). The final step of 40S ribosomal subunit maturation is controlled by a dual key lock. *eLife*, *10*, e61254. https://doi.org/10.7554/eLife.61254

Preti, M., O'Donohue, M.-F., Montel-Lehry, N., Bortolin-Cavaille, M.-L., Choesmel, V., & Gleizes, P.-E. (2013). Gradual processing of the ITS1 from the nucleolus to the cytoplasm during synthesis of the human 18S rRNA. *Nucleic Acids Research*, *41*(8), 4709–4723. https://doi.org/10.1093/nar/gkt160

Rai, J., Parker, M. D., Huang, H., Choy, S., Ghalei, H., Johnson, M. C., Karbstein, K., & Stroupe, M. E. (2021). An open interface in the pre-80S ribosome coordinated by ribosome assembly factors Tsr1 and Dim1 enables temporal regulation of Fap7. *RNA*, *27*(2), 221–233. https://doi.org/10.1261/rna.077610.120

Ridanpää, M., van Eenennaam, H., Pelin, K., Chadwick, R., Johnson, C., Yuan, B., van Venrooij, W., Pruijn, G., Salmela, R., Rockas, S., Mäkitie, O., Kaitila, I., & de la Chapelle, A. (2001). Mutations in the RNA component of RNase MRP cause a pleiotropic human disease, cartilage-hair hypoplasia. *Cell*, *104*(2), 195–203. https://doi.org/10.1016/s0092-8674(01)00205-7

Robertson, N., Shchepachev, V., Wright, D., Turowski, T. W., Spanos, C., Helwak, A., Zamoyska, R., & Tollervey, D. (2022). A disease-linked lncRNA mutation in RNase MRP inhibits ribosome synthesis. *Nature Communications*, *13*(1), 649. https://doi.org/10.1038/s41467-022-28295-8

Sailer, C., Jansen, J., Sekulski, K., Cruz, V. E., Erzberger, J. P., & Stengel, F. (2022). A comprehensive landscape of 60S ribosome biogenesis factors. *Cell Reports*, *38*(6), 110353. https://doi.org/10.1016/j.celrep.2022.110353

Sakamoto, M., Iwama, K., Sekiguchi, F., Mashimo, H., Kumada, S., Ishigaki, K., Okamoto, N., Behnam, M., Ghadami, M., Koshimizu, E., Miyatake, S., Mitsuhashi, S., Mizuguchi, T., Takata, A., Saitsu, H., Miyake, N., & Koshimizu, E. (2021). Novel EXOSC9 variants cause pontocerebellar hypoplasia type 1D with spinal motor neuronopathy and cerebellar atrophy. *Journal of Human Genetics*, *66*, 401–407. https://doi.org/10.1038/s10038-020-00853-2

Scaiola, A., Peña, C., Weisser, M., Böhringer, D., Leibundgut, M., Klingauf-Nerurkar, P., Gerhardy, S., Panse, V. G., & Ban, N. (2018). Structure of a eukaryotic cytoplasmic pre-40S ribosomal subunit. *The EMBO Journal*, *37*(7), e98499. https://doi.org/10.15252/embj.201798499

Schaeffer, D., Tsanova, B., Barbas, A., Reis, F. P., Dastidar, E. G., Sanchez-Rotunno, M., Arraiano, C. M., & van Hoof, A. (2009). The exosome contains domains with specific endoribonuclease, exoribonuclease and cytoplasmic mRNA decay activities. *Nature Structural & Molecular Biology*, *16*(1), 56–62. https://doi.org/10.1038/nsmb.1528

Schilders, G., van Dijk, E., & Pruijn, G. J. M. (2007). C1D and hMtr4p associate with the human exosome subunit PM/Scl-100 and are involved in pre-rRNA processing. *Nucleic Acids Research*, *35*(8), 2564–2572. https://doi.org/10.1093/nar/gkm082

Schillewaert, S., Wacheul, L., Lhomme, F., & Lafontaine, D. L. J. (2012). The evolutionarily conserved protein Las1 is required for pre-rRNA processing at both ends of ITS2. *Molecular and Cellular Biology*, *32*(2), 430–444. https://doi.org/10.1128/MCB.06019-11

Schmitt, M. E., & Clayton, D. A. (1993). Nuclear RNase MRP is required for correct processing of pre-5.8S rRNA in Saccharomyces cerevisiae. *Molecular and Cellular Biology*, *13*(12), 7935–7941. https://doi.org/10.1128/mcb.13.12.7935-7941.1993

Schneider, C., Anderson, J. T., & Tollervey, D. (2007). The exosome subunit Rrp44 plays a direct role in RNA substrate recognition. *Molecular Cell*, *27*(2), 324–331. https://doi.org/10.1016/j.molcel.2007.06.006

Schneider, C., Kudla, G., Wlotzka, W., Tuck, A., & Tollervey, D. (2012). Transcriptome-wide analysis of exosome targets. *Molecular Cell*, *48*(3), 422–433. https://doi.org/10.1016/j.molcel.2012.08.013

Schneider, C., Leung, E., Brown, J., & Tollervey, D. (2009). The N-terminal PIN domain of the exosome subunit Rrp44 harbors endonuclease activity and tethers Rrp44 to the yeast core exosome. *Nucleic Acids Research*, *37*(4), 1127–1140. https://doi.org/10.1093/nar/gkn1020

Schneider, C., & Tollervey, D. (2013). Threading the barrel of the RNA exosome. *Trends in Biochemical Sciences*, *38*(10), 485–493. https://doi.org/10.1016/j.tibs.2013.06.013

Schneider, C., & Tollervey, D. (2014). Looking into the barrel of the RNA exosome. *Nature Structural and Molecular Biology*, *21*(1), 17–18. https://doi.org/10.1038/nsmb.2750

Schuch, B., Feigenbutz, M., Makino, D. L., Falk, S., Basquin, C., Mitchell, P., & Conti, E. (2014). The exosome-binding factors Rrp6 and Rrp47 form a composite surface for recruiting the Mtr4 helicase. *The EMBO Journal*, *33*(23), 2829–2846. https://doi.org/10.15252/embj.201488757

Schuller, J. M., Falk, S., Fromm, L., Hurt, E., & Conti, E. (2018). Structure of the nuclear exosome captured on a maturing preribosome. *Science*, *360*(6385), 219–222. https://doi.org/10.1126/science.aar5428

Scott, D. D., Trahan, C., Zindy, P. J., Aguilar, L. C., Delubac, M. Y., Van Nostrand, E. L., Adivarahan, S., Wei, K. E., Yeo, G. W., Zenklusen, D., & Oeffinger, M. (2017). Nol12 is a multifunctional RNA binding protein at the nexus of RNA and DNA metabolism. *Nucleic Acids Research*, *45*(21), 12509–12528. https://doi.org/10.1093/nar/gkx963

Shayan, R., Rinaldi, D., Larburu, N., Plassart, L., Balor, S., Bouyssié, D., Lebaron, S., Marcoux, J., Gleizes, P. E., & Plisson-Chastang, C. (2020). Good vibrations: Structural remodeling of maturing yeast pre-40S ribosomal particles followed by cryo-electron microscopy. *Molecules*, *25*(5), 1125. https://doi.org/10.3390/molecules25051125

Singh, S., Vanden Broeck, A., Miller, L., Chaker-Margot, M., & Klinge, S. (2021). Nucleolar maturation of the human small subunit processome. *Science*, *373*(6560), eabj5338. https://doi.org/10.1126/science.abj5338

Slavotinek, A., Misceo, D., Htun, S., Mathisen, L., Frengen, E., Foreman, M., Hurtig, J. E., Enyenihi, L., Sterrett, M. C., Leung, S. W., Schneidman-Duhovny, D., Estrada-Veras, J., Duncan, J. L., Haaxma, C. A., Kamsteeg, E. J., Xia, V., Beleford, D., Si, Y., Douglas, G., … Corbett, A. H. (2020). Biallelic variants in the RNA exosome gene EXOSC5 are associated with developmental delays, short stature, cerebellar hypoplasia and motor weakness. *Human Molecular Genetics*, *29*(13), 2218–2239. https://doi.org/10.1093/hmg/ddaa108

Sloan, K. E., Bohnsack, M. T., Schneider, C., & Watkins, N. J. (2014). The roles of SSU processome components and surveillance factors in the initial processing of human ribosomal RNA. *RNA*, *20*(4), 540–550. https://doi.org/10.1261/rna.043471.113

Sloan, K. E., Mattijssen, S., Lebaron, S., Tollervey, D., Pruijn, G. J. M., & Watkins, N. J. (2013). Both endonucleolytic and exonucleolytic cleavage mediate ITS1 removal during human ribosomal RNA processing. *The Journal of Cell Biology*, *200*(5), 577–588. https://doi.org/10.1083/jcb.201207131

Sloan, K. E., Schneider, C., & Watkins, N. J. (2012). Comparison of the yeast and human nuclear exosome complexes. *Biochemical Society Transactions*, *40*(4), 850–855. https://doi.org/10.1042/BST20120061

Sloan, K. E., Knox, A. A., Wells, G. R., Schneider, C., & Watkins, N. J. (2019). Interactions and activities of factors involved in the late stages of human 18S rRNA maturation. *RNA Biology*, *16*(2), 196–210. https://doi.org/10.1080/15476286.2018.1564467

Somashekar, P. H., Kaur, P., Stephen, J., Guleria, V. S., Kadavigere, R., Girisha, K. M., Bielas, S., Upadhyai, P., & Shukla, A. (2021). Bi-allelic missense variant, p . Ser35Leu in EXOSC1 is associated with pontocerebellar hypoplasia. *Clinical Genetics*, *99*, 594–600. https://doi.org/10.1111/cge.13928

Song, H., Fang, X., Jin, L., Shaw, G. X., Wang, Y. X., & Ji, X. (2017). The functional cycle of Rnt1p: Five consecutive steps of double-stranded RNA processing by a eukaryotic RNase III. *Structure*, *25*(2), 353–363. https://doi.org/10.1016/j.str.2016.12.013

Staals, R. H. J., Bronkhorst, A. W., Schilders, G., Slomovic, S., Schuster, G., Heck, A. J. R., Raijmakers, R., & Pruijn, G. J. M. (2010). Dis3-like 1: A novel exoribonuclease associated with the human exosome. *The EMBO Journal*, *29*(14), 2358–2367. https://doi.org/10.1038/emboj.2010.122

Stembalska, A., Rydzanicz, M., Walas, W., Gasperowicz, P., Pollak, A., Pienkowski, V. M., Biela, M., Klaniewska, M., Gamrot, Z., Gronska, E., Ploski, R., & Smigiel, R. (2022). Severe infantile axonal neuropathy with respiratory failure caused by novel mutation in X-linked *LAS1L* gene. *Genes*, *13*(5), 725. https://doi.org/10.3390/genes13050725

Strunk, B. S., Novak, M. N., Young, C. L., & Karbstein, K. (2012). A translation-like cycle is a quality control checkpoint for maturing 40S ribosome subunits. *Cell*, *150*(1), 111–121. https://doi.org/10.1016/j.cell.2012.04.044

Stuart, B. D., Choi, J., Zaidi, S., Xing, C., Holohan, B., Chen, R., Choi, M., Dharwadkar, P., Torres, F., Girod, C. E., Weissler, J., Fitzgerald, J., Kershaw, C., Klesney-Tait, J., Mageto, Y., Shay, J. W., Ji, W., Bilguvar, K., Mane, S., … Garcia, C. K. (2015). Exome sequencing links mutations in PARN and RTEL1 with familial pulmonary fibrosis and telomere shortening. *Nature Genetics*, *47*(5), 512–517. https://doi.org/10.1038/ng.3278

Sun, Q., Zhu, X., Qi, J., An, W., Lan, P., Tan, D., Chen, R., Wang, B., Zheng, S., Zhang, C., Chen, X., Zhang, W., Chen, J., Dong, M. Q., & Ye, K. (2017). Molecular architecture of the 90S small subunit pre-ribosome. *eLife*, *6*, e22086. https://doi.org/10.7554/eLife.22086

Szczepińska, T., Kalisiak, K., Tomecki, R., Labno, A., Borowski, L. S., Kulinski, T. M., Adamska, D., Kosinska, J., & Dziembowski, A. (2015). DIS3 shapes the RNA polymerase II transcriptome in humans by degrading a variety of unwanted transcripts. *Genome Research*, *25*(11), 1622–1633. https://doi.org/10.1101/gr.189597.115

Tafforeau, L., Zorbas, C., Langhendries, J.-L., Mullineux, S.-T., Stamatopoulou, V., Mullier, R., Wacheul, L., & Lafontaine, D. L. J. (2013). The complexity of human ribosome biogenesis revealed by systematic nucleolar screening of pre-rRNA processing factors. *Molecular Cell*, *51*(4), 539–551. https://doi.org/10.1016/j.molcel.2013.08.011

Tan, D., Marzluff, W. F., Dominski, Z., & Tong, L. (2013). Structure of histone mRNA stem-loop, human stem-loop binding protein, and 3′hExo ternary complex. *Science*, *339*(6117), 318–321. https://doi.org/10.1126/science.1228705

Tanaka, N., Smith, P., & Shuman, S. (2011). Crystal structure of Rcl1, an essential component of the eukaryal pre-rRNA processosome implicated in 18s rRNA biogenesis. *RNA*, *17*(4), 595–602. https://doi.org/10.1261/rna.2571811

Tesina, P., Heckel, E., Cheng, J., Fromont-Racine, M., Buschauer, R., Kater, L., Beatrix, B., Berninghausen, O., Jacquier, A., Becker, T., & Beckmann, R. (2019). Structure of the 80S ribosome-Xrn1 nuclease complex. *Nature Structural & Molecular Biology*, *26*(4), 275–280. https://doi.org/10.1038/s41594-019-0202-5

Thiel, C. T., Horn, D., Zabel, B., Ekici, A. B., Salinas, K., Gebhart, E., Rüschendorf, F., Sticht, H., Spranger, J., Müller, D., Zweier, C., Schmitt, M. E., Reis, A., & Rauch, A. (2005). Severely incapacitating mutations in patients with extreme short stature identify RNA-processing endoribonuclease RMRP as an essential cell growth regulator. *American Journal of Human Genetics*, *77*(5), 795–806. https://doi.org/10.1086/497708

Thoms, M., Thomson, E., Baßler, J., Gnädig, M., Griesel, S., & Hurt, E. (2015). The exosome is recruited to RNA substrates through specific adaptor proteins. *Cell*, *162*(5), 1029–1038. https://doi.org/10.1016/j.cell.2015.07.060

Thomson, E., & Tollervey, D. (2005). Nop53p is required for late 60S ribosome subunit maturation and nuclear export in yeast. *RNA*, *11*(8), 1215–1224. https://doi.org/10.1261/rna.2720205

Thomson, E., & Tollervey, D. (2010). The final step in 5.8S rRNA processing is cytoplasmic in Saccharomyces cerevisiae. *Molecular and Cellular Biology*, *30*(4), 976–984. https://doi.org/10.1128/MCB.01359-09

Tomecki, R., Drazkowska, K., Kucinski, I., Stodus, K., Szczesny, R. J., Gruchota, J., Owczarek, E. P., Kalisiak, K., & Dziembowski, A. (2014). Multiple myeloma-associated hDIS3 mutations cause perturbations in cellular RNA metabolism and suggest hDIS3 PIN domain as a potential drug target. *Nucleic Acids Research*, *42*(2), 1270–1290. https://doi.org/10.1093/nar/gkt930

Tomecki, R., Kristiansen, M. S., Lykke-Andersen, S., Chlebowski, A., Larsen, K. M., Szczesny, R. J., Drazkowska, K., Pastula, A., Andersen, J. S., Stepien, P. P., Dziembowski, A., & Jensen, T. H. (2010). The human core exosome interacts with differentially localized processive RNases: hDIS3 and hDIS3L. *The EMBO Journal*, *29*(14), 2342–2357. https://doi.org/10.1038/emboj.2010.121

Tomecki, R., Labno, A., Drazkowska, K., Cysewski, D., & Dziembowski, A. (2015). hUTP24 is essential for processing of the human rRNA precursor at site A1, but not at site A0. *RNA Biology*, *12*(9), 1010–1029. https://doi.org/10.1080/15476286.2015.1073437

Tomecki, R., Sikorski, P. J., & Zakrzewska-Placzek, M. (2017). Comparison of preribosomal RNA processing pathways in yeast, plant and human cells—Focus on coordinated action of endo- and exoribonucleases. *FEBS Letters*, *591*(13), 1801–1850. https://doi.org/10.1002/1873-3468.12682

Tummala, H., Walne, A., Collopy, L., Cardoso, S., de la Fuente, J., Lawson, S., Powell, J., Cooper, N., Foster, A., Mohammed, S., Plagnol, V., Vulliamy, T., & Dokal, I. (2015). Poly(A)-specific ribonuclease deficiency impacts telomere biology and causes dyskeratosis congenita. *The Journal of Clinical Investigation*, *125*(5), 2151–2160. https://doi.org/10.1172/JCI78963

Tunyasuvunakool, K., Adler, J., Wu, Z., Green, T., Zielinski, M., Žídek, A., Bridgland, A., Cowie, A., Meyer, C., Laydon, A., Velankar, S., Kleywegt, G. J., Bateman, A., Evans, R., Pritzel, A., Figurnov, M., Ronneberger, O., Bates, R., Kohl, S. A. A., ... Hassabis, D. (2021). Highly accurate protein structure prediction for the human proteome. *Nature*, *596*(7873), 590–596. https://doi.org/10.1038/s41586-021-03828-1

Turowski, T. W., Lebaron, S., Zhang, E., Peil, L., Dudnakova, T., Petfalski, E., Granneman, S., Rappsilber, J., & Tollervey, D. (2014). Rio1 mediates ATP-dependent final maturation of 40S ribosomal subunits. *Nucleic Acids Research*, *42*(19), 12189–12199. https://doi.org/10.1093/nar/gku878

van Hoof, A., Lennertz, P., & Parker, R. (2000). Three conserved members of the RNase D family have unique and overlapping functions in the processing of 5S, 5.8S, U4, U5, RNase MRP and RNase P RNAs in yeast. *The EMBO Journal*, *19*(6), 1357–1365. https://doi.org/10.1093/emboj/19.6.1357

Vanden Broeck, A., & Klinge, S. (2022). An emerging mechanism for the maturation of the small subunit processome. *Current Opinion in Structural Biology*, *73*, 102331. https://doi.org/10.1016/j.sbi.2022.102331

Walker, S. C., & Engelke, D. R. (2006). Ribonuclease P: The evolution of an ancient RNA enzyme. *Critical Reviews in Biochemistry and Molecular Biology*, *41*(2), 77–102. https://doi.org/10.1080/10409230600602634

Wan, J., Yourshaw, M., Mamsa, H., Rudnik-Schöneborn, S., Menezes, M. P., Hong, J. E., Leong, D. W., Senderek, J., Salman, M. S., Chitayat, D., Seeman, P., von Moers, A., Graul-Neumann, L., Kornberg, A. J., Castro-Gago, M., Sobrido, M. J., Sanefuji, M., Shieh, P. B., Salamon, N., ... Jen, J. C. (2012). Mutations in the RNA exosome component gene EXOSC3 cause pontocerebellar hypoplasia and spinal motor neuron degeneration. *Nature Genetics*, *44*(6), 704–708. https://doi.org/10.1038/ng.2254

Wasmuth, E. V., Januszyk, K., & Lima, C. D. (2014). Structure of an Rrp6-RNA exosome complex bound to poly(A) RNA. *Nature*, *511*(7510), 435–439. https://doi.org/10.1038/nature13406

Wasmuth, E. V., Zinder, J. C., Zattas, D., Das, M., & Lima, C. D. (2017). Structure and reconstitution of yeast Mpp6-nuclear exosome complexes reveals that Mpp6 stimulates RNA decay and recruits the Mtr4 helicase. *eLife*, *6*, e29062. https://doi.org/10.7554/eLife.29062

Weick, E.-M., & Lima, C. D. (2021). RNA helicases are hubs that orchestrate exosome-dependent 3′-5′ decay. *Current Opinion in Structural Biology*, *67*, 86–94. https://doi.org/10.1016/j.sbi.2020.09.010

Weick, E.-M., Puno, M. R., Januszyk, K., Zinder, J. C., DiMattia, M. A., & Lima, C. D. (2018). Helicase-dependent RNA decay illuminated by a Cryo-EM structure of a human nuclear RNA exosome-MTR4 complex. *Cell*, *173*(7), 1663–1677.e21. https://doi.org/10.1016/j.cell.2018.05.041

Weir, J. R., Bonneau, F., Hentschel, J., & Conti, E. (2010). Structural analysis reveals the characteristic features of Mtr4, a DExH helicase involved in nuclear RNA processing and surveillance. *Proceedings of the National Academy of Sciences of the United States of America*, *107*(27), 12139–12144. https://doi.org/10.1073/pnas.1004953107

Wells, G. R., Weichmann, F., Colvin, D., Sloan, K. E., Kudla, G., Tollervey, D., Watkins, N. J., & Schneider, C. (2016). The PIN domain endonuclease Utp24 cleaves pre-ribosomal RNA at two coupled sites in yeast and humans. *Nucleic Acids Research*, *44*(11), 5399–5409. https://doi.org/10.1093/nar/gkw213

Wells, G. R., Weichmann, F., Sloan, K. E., Colvin, D., Watkins, N. J., & Schneider, C. (2017). The ribosome biogenesis factor yUtp23/hUTP23 coordinates key interactions in the yeast and human pre-40S particle and hUTP23 contains an essential PIN domain. *Nucleic Acids Research*, *45*(8), 4796–4809. https://doi.org/10.1093/nar/gkw1344

Wilson, M., Mulley, J., Gedeon, A., Robinson, H., & Turner, G. (1991). New X-linked syndrome of mental retardation, gynecomastia, and obesity is linked to DXS255. *American Journal of Medical Genetics*, *40*(4), 406–413. https://doi.org/10.1002/ajmg.1320400405

Wu, M., Nilsson, P., Henriksson, N., Niedzwiecka, A., Lim, M. K., Cheng, Z., Kokkoris, K., Virtanen, A., & Song, H. (2009). Structural basis of m7GpppG binding to poly(A)-specific ribonuclease. *Structure*, *17*(2), 276–286. https://doi.org/10.1016/j.str.2008.11.012

Wu, M., Reuter, M., Lilie, H., Liu, Y., Wahle, E., & Song, H. (2005). Structural insight into poly(A) binding and catalytic mechanism of human PARN. *EMBO Journal*, *24*(23), 4082–4093. https://doi.org/10.1038/sj.emboj.7600869

Wu, S., Tan, D., Woolford, J. L. J., Dong, M.-Q., & Gao, N. (2017). Atomic modeling of the ITS2 ribosome assembly subcomplex from cryo-EM together with mass spectrometry-identified protein-protein crosslinks. *Protein Science*, *26*(1), 103–112. https://doi.org/10.1002/pro.3045

Xiang, S., Cooper-Morgan, A., Jiao, X., Kiledjian, M., Manley, J. L., & Tong, L. (2009). Structure and function of the 5′→3′ exoribonuclease Rat1 and its activating partner Rai1. *Nature*, *458*(7239), 784–788. https://doi.org/10.1038/nature07731

Zhang, L., Wu, C., Cai, G., Chen, S., & Ye, K. (2016). Stepwise and dynamic assembly of the earliest precursors of small ribosomal subunits in yeast. *Genes & Development*, *30*(6), 718–732. https://doi.org/10.1101/gad.274688.115

Zinder, J. C., & Lima, C. D. (2017). Targeting RNA for processing or destruction by the eukaryotic RNA exosome and its cofactors. *Genes & Development*, *31*(2), 88–100. https://doi.org/10.1101/gad.294769.116

Zinder, J. C., Wasmuth, E. V., & Lima, C. D. (2016). Nuclear RNA exosome at 3.1 Å reveals substrate specificities, RNA paths, and allosteric inhibition of Rrp44/Dis3. *Molecular Cell*, *64*(4), 734–745. https://doi.org/10.1016/j.molcel.2016.09.038

How to cite this article: Schneider, C., & Bohnsack, K. E. (2023). Caught in the act—Visualizing ribonucleases during eukaryotic ribosome assembly. *WIREs RNA*, *14*(4), e1766. https://doi.org/10.1002/wrna.1766